

University of Windsor

Scholarship at UWindor

Electronic Theses and Dissertations

Theses, Dissertations, and Major Papers

1-1-2007

A comparison of the kinematic response and biofidelity of the neck of pediatric cadaver data and the Hybrid III three-year-old child finite element model.

Miroslav Joseph Tot
University of Windsor

Follow this and additional works at: <https://scholar.uwindsor.ca/etd>

Recommended Citation

Tot, Miroslav Joseph, "A comparison of the kinematic response and biofidelity of the neck of pediatric cadaver data and the Hybrid III three-year-old child finite element model." (2007). *Electronic Theses and Dissertations*. 7043.

<https://scholar.uwindsor.ca/etd/7043>

This online database contains the full-text of PhD dissertations and Masters' theses of University of Windsor students from 1954 forward. These documents are made available for personal study and research purposes only, in accordance with the Canadian Copyright Act and the Creative Commons license—CC BY-NC-ND (Attribution, Non-Commercial, No Derivative Works). Under this license, works must always be attributed to the copyright holder (original author), cannot be used for any commercial purposes, and may not be altered. Any other use would require the permission of the copyright holder. Students may inquire about withdrawing their dissertation and/or thesis from this database. For additional inquiries, please contact the repository administrator via email (scholarship@uwindsor.ca) or by telephone at 519-253-3000ext. 3208.

**A COMPARISON OF THE KINEMATIC RESPONSE AND
BIOFIDELITY OF THE NECK OF PEDIATRIC CADAVER DATA
AND THE HYBRID III THREE-YEAR-OLD CHILD
FINITE ELEMENT MODEL**

by

Miroslav Joseph Tot

A Thesis

**Submitted to the Faculty of Graduate Studies
through Kinesiology
in Partial Fulfillment of the Requirements for
the Degree of Master of Human Kinetics at the
University of Windsor**

Windsor, Ontario, Canada

2007

© 2007 Miroslav Joseph Tot



Library and
Archives Canada

Bibliothèque et
Archives Canada

Published Heritage
Branch

Direction du
Patrimoine de l'édition

395 Wellington Street
Ottawa ON K1A 0N4
Canada

395, rue Wellington
Ottawa ON K1A 0N4
Canada

Your file *Votre référence*
ISBN: 978-0-494-35174-1
Our file *Notre référence*
ISBN: 978-0-494-35174-1

NOTICE:

The author has granted a non-exclusive license allowing Library and Archives Canada to reproduce, publish, archive, preserve, conserve, communicate to the public by telecommunication or on the Internet, loan, distribute and sell theses worldwide, for commercial or non-commercial purposes, in microform, paper, electronic and/or any other formats.

The author retains copyright ownership and moral rights in this thesis. Neither the thesis nor substantial extracts from it may be printed or otherwise reproduced without the author's permission.

AVIS:

L'auteur a accordé une licence non exclusive permettant à la Bibliothèque et Archives Canada de reproduire, publier, archiver, sauvegarder, conserver, transmettre au public par télécommunication ou par l'Internet, prêter, distribuer et vendre des thèses partout dans le monde, à des fins commerciales ou autres, sur support microforme, papier, électronique et/ou autres formats.

L'auteur conserve la propriété du droit d'et des droits moraux qui protège cette thèse. Ni la thèse ni des extraits substantiels de celle-ci ne doivent être imprimés ou autrement reproduits sans son autorisation.

In compliance with the Canadian Privacy Act some supporting forms may have been removed from this thesis.

Conformément à la loi canadienne sur la protection de la vie privée, quelques formulaires secondaires ont été enlevés de cette thèse.

While these forms may be included in the document page count, their removal does not represent any loss of content from the thesis.

Bien que ces formulaires aient inclus dans la pagination, il n'y aura aucun contenu manquant.


Canada

ABSTRACT

This research focuses on comparing the kinematic response of the head and neck of the Hybrid III three-year-old anthropometric test device finite element model and pediatric cadaver data under tensile distraction and flexion-extension bending loading conditions. In this work, an explicit finite element code (LS-DYNA) and the Hybrid III finite element model were used to numerically simulate previous experimental cadaver tests. Significant differences in linear and rotational stiffness were found between the Hybrid III and the pediatric cadaver data. The pediatric cadaver data was implemented into the Hybrid III model and loaded with a crash pulse obtained from experimental child cadaver sled test. Comparisons of kinematic were made and it was found that the altered model exhibited a 31 percent greater degree of head rotation, a 141 percent greater degree of chest deflection, and the head trajectory more closely resembled that of the experimental pediatric cadaver sled test.

DEDICATION

For my loving wife Coleen, who has offered unconditional love and support throughout the course of this project and to all of the people in my life that have inspired, encouraged and motivated me to pursue higher education.

ACKNOWLEDGEMENTS

The author would like to thank his academic advisor, Dr. Wayne Marino, for his confidence in my ability and patience to see this project through. In addition, I am grateful for the assistance provided by the committee, namely, Dr. William Altenhof with the technical aspects of the research and for sharing with me his immense knowledge of vehicle crashworthiness and finite element analysis and Dr. Kenji Kenno for his contributions to this paper. I would also like to thank Dr. Jun Ouyang of the Southern Medical University of Guangzhou China for making available his pediatric cadaver research. As well, a special thanks to Ms. Tanya Kapoor for her assistance with finite element modeling.

TABLE OF CONTENTS

	Page
ABSTRACT	iii
DEDICATION	iv
ACKNOWLEDGEMENTS	v
LIST OF FIGURES	ix
LIST OF APPENDICES	xi
LIST OF ABBREVIATIONS	xii
LIST OF NOMENCLATURE	xiv
1. INTRODUCTION	1
1.1 Statement of the Problem	1
1.2 Operating Definitions	3
1.3 Hypotheses	4
2. LITERATURE REVIEW	5
2.1 Automotive Crash Statistics	5
2.1.1 Canada.....	5
2.1.2 United States	5
2.2 Injury	6
2.2.1 Patterns of Injury.....	6
2.2.2 Case Studies.....	7
2.3 Injury Mechanism and Biomechanics	11
2.3.1 CRS as a Mechanism to Reduce Injury	11
2.3.2 Velocity and Time Duration as Injury Mechanisms.....	11
2.3.3 Pediatric Cervical Spine Anatomy.....	12
2.3.4 Biomechanics of the Pediatric Cervical Spine.....	14
2.3.5 Resultant Mechanism of Injury and AOD	15
2.4 Head and Neck Injury	16
2.4.1 Head Injury	16
2.4.2 Neck Injury	18
2.4.3 Chest Injury.....	20

2.5 Overview of Testing Methodologies Applicable to the Problem	20
2.5.1 Experimental	20
2.5.2 Theoretical	24
2.5.3 Numerical.....	25
3. FOCUS OF RESEARCH	29
3.1 Limitations of the Proposed Study	30
4. EXPERIMENTAL PROCEDURE OR METHODS	32
4.1 Experimental Procedure	32
4.2 Numerical Procedures	33
4.2.1 Preparation of the Finite Element Model Head-Neck Complex.....	33
4.2.2 Extraction of Data from the Hybrid III Finite Element Model.....	34
4.2.3 Incorporation of the Pediatric Data into the Finite Element Model.....	35
5. RESULTS	37
5.1 Head and Neck Component Test Analysis.....	37
5.1.1 Linear Stiffness	37
5.1.2 Angular Stiffness	39
5.2 Qualitative Kinematic Crash Analysis.....	41
5.3 Quantitative Kinematic Crash Analysis	44
5.3.1 Head Acceleration.....	44
5.3.2 Chest Acceleration	47
5.3.3 Chest Deflection.....	50
5.3.4 Neck Forces	51
5.3.5 Neck Moments	53
5.3.6 Head Injury Criteria.....	55
5.3.7 Head Rotation	56
5.3.8 Head Trajectory	57
6. DISCUSSION	59
6.1 Head and Neck Component Test Analysis.....	59
6.1.1 Linear Stiffness	59
6.1.2 Angular Stiffness	59

6.2 Qualitative Kinematic Crash Analysis	61
6.3 Quantitative Kinematic Crash Analysis	61
6.3.1 Head Acceleration.....	61
6.3.2 Chest Acceleration.....	62
6.3.3 Chest Deflection.....	62
6.3.4 Neck Forces	63
6.3.5 Neck Moments	64
6.3.6 Head Injury Criteria.....	65
6.3.7 Head Rotation	66
6.3.8 Head Trajectory	66
6.4 Hypotheses Revisited	67
6.4.1 Hypothesis.....	67
6.4.2 Hypothesis 2.....	67
6.4.3 Hypothesis 3.....	68
6.4.4 Null Hypothesis	68
7. CONCLUSIONS AND FUTURE WORK	69
7.1 Conclusions.....	69
7.2 Future Work.....	70
8. PUBLICATIONS RESULTING FROM THIS WORK	71
9. REFERENCES	72
10. APPENDICES	81
APPENDIX A	81
The Finite Element Method	81
APPENDIX B	82
Abbreviated Injury Scale	82
11. VITA AUCTORIS	83

LIST OF FIGURES

Figure	Page
Figure 1. Accident reconstruction diagram.....	8
Figure 2. Case vehicle, a 1994 SUV	8
Figure 3. Slight hemmorrhage at the tectorial membrane	9
Figure 4. Posterior view of the Occ-C2 complex and tectorial membrane.....	13
Figure 5. Medial sagittal plane of the Occ-C2 complex	14
Figure 6. Axial neck force load-deflection curve for altered, unaltered and peditric data.	38
Figure 7. Axial neck force load-deflection curve for altered and peditric data	39
Figure 8. Angular neck moment load vs. deflection curve for altered, unaltered and peditric data under flexion and extension bending	40
Figure 9. Angular neck moment load vs. deflection curve for altered and peditric data under flexion and extension bending	41
Figure 10. Frame by frame comparative analysis of altered vs. unaltered models.....	42
Figure 11. Cross sectional comparative analysis of altered vs. unaltered models.....	43
Figure 12. Head acceleration in the local x direction	45
Figure 13. Head acceleration in the local z direction.....	46
Figure 14. Resultant head acceleration	47
Figure 15. Chest acceleration in the local x direction.....	48
Figure 16. Chest acceleration in the local z direction.....	49
Figure 17. Resultant chest acceleration.....	50
Figure 18. Chest deflection	51
Figure 19. Resultant upper neck force	52
Figure 20. Resultant lower neck force	53

Figure 21. Resultant upper neck moment	54
Figure 22. Resultant lower neck moment	55
Figure 23. Head injury criteria.....	56
Figure 24. Head rotation	57
Figure 25. Head trajectory	58

LIST OF APPENDICES

APPENDIX A	The Finite Element Method
APPENDIX B	The Abbreviated Injury Scale

LIST OF ABBREVIATIONS

AIS	Abbreviated Injury Scale
AOD	Atlantooccipital Dislocation
ATD	Anthropometric Test Device
CAD	Computer Assisted Design
CIREN	Crash Injury Research Engineering Network
CMVSS	Canadian Motor Vehicle Safety Standard
CRS	Child Restraint System
CTI	Combined Thoracic Index
FEA	Finite Element Analysis
FEM	Finite Element Model
FEMB	Finite Element Model Builder
FMVSS	Federal Motor Vehicle Safety Standard
GSI	Gad Severity Index
HIC	Head Injury Criterion
IIHS	Insurance Institute for Highway Safety
IARV	Injury Assessment Reference Values
ISO	International Standards Organization
LATCH	Lower Anchors and Tethers for Children
MVC	Motor Vehicle Crash
NASA	National Aeronautics and Space Administration
NCSA	National Centre for Statistics and Analysis
NHTSA	National Highway Traffic Safety Administration

NIC	Neck Injury Criteria
Nij	Normalized Neck Injury Criteria
Occ-C2	Occipitoatlantoaxial
SUV	Sport Utility Vehicle
THUMS	Total Human Model for Safety
TSI	Traumatic Spinal Injury
WSTC	Wayne State Tolerance Curve

LIST OF NOMENCLATURE

a	Acceleration (m/s^2)
C1	First cervical vertebrae
C2	Second cervical vertebrae
C3	Third cervical vertebrae
C4	Fourth cervical vertebrae
C5	Fifth cervical vertebrae
C6	Sixth cervical vertebrae
C7	Seventh cervical vertebrae
k	Stiffness (N/m)
T1	First thoracic vertebrae
T2	Second thoracic vertebrae
Occ	Occiput
v	Velocity (m/s)

1. INTRODUCTION

1.1 Statement of the Problem

Motor vehicle accidents are the third leading cause of premature death and long term disability for persons of all age groups in Canada. In 2001, Transport Canada reported 2,778 deaths due to motor vehicle accidents, 24,403 hospital admissions and a total estimated annual cost of \$25 billion dollars (Transport Canada, 2004). In the same year, 523 child fatalities were attributed to transport accidents (Statistics Canada, 2006). Motor vehicle accidents are the leading cause of death for children in Canada (Statistics Canada, 2003).

Similarly, in the United States, the National Highway Traffic Safety Administration (NHTSA) has found that motor vehicle accidents are the leading cause of death for persons aged 3 through 34. When measured by years of life lost, motor vehicle accidents rank third as cause of death for all age groups, trailing behind only cancer and cardiovascular disease. The number of years of life lost measure highlights the disproportionate impact motor vehicle accidents have on the younger demographic of the population. It is evident from these statistics that the younger population is at an increased risk of death and loss of life expectancy (NHTSA, 2006).

Williamson, Irvine, & Sadural, (2002) found that children in the 3 to 4 year age group account for a greater number of passenger fatalities (45.5 percent) than any other age group. The most common body part injured for children involved in motor vehicle frontal impact crashes is the head and the neck, followed by injuries of the torso and extremities (King, 2000). Injuries to the head and neck account for a greater number and severity of abbreviated injury scale (AIS) 2+ injuries (Arbogast, Cornejo, Kallan,

Winston, & Durbin, 2002). When ranked by specific age, motor vehicle accidents are the leading cause of death for children aged 3 years old (NHTSA, 2006).

Research and development on child occupant crash protection relies heavily on the biofidelity of anthropomorphic test devices (ATD's) and the ability to relate measured parameters on the ATD to injury (Yannacome, Whitman, Sicher, & D'Aulerio, 2005). The Hybrid III three-year-old ATD is the only official device recognized by the International Standards Organization (ISO), NHTSA, Insurance Institute for Highway Safety (IIHS), Transport Canada and European regulations for frontal impact compliance testing (General Motors, 2006). In previous studies comparing the head-neck responses of the Hybrid III adult-male ATD and adult human cadaver, the neck of the Hybrid III adult-male ATD was found to be between 2 and 4 times stiffer and transmitted approximately 48.5 percent more force to the lower neck under axial compression as compared to the adult human cadaver (Sances & Kumaresan 2001; Sances, Carlin & Kumaresan, 2002). In addition it has been shown that the thoracic spine of the Hybrid III six-year-old ATD is overly stiff and results in high neck forces and moments that are not representative of the true injury potential (Sherwood, Shaw, Van Rooij, Kent, Crandall, Orzechowski, Eichelberger, & Kallieris 2003).

There have been no documented studies comparing the stiffness of the Hybrid III three-year-old ATD model neck under axial tensile loading and flexion to human pediatric cadaver tests. However, previous research suggests that there is a strong need for improving the biofidelity of the neck of the Hybrid III three-year-old child ATD model. Therefore, the specific purpose of the proposed study is to compare the kinematic neck response of the Hybrid III three-year-old child finite element model with known

real-life pediatric cadaver data from three-year-old subjects. The biomechanical response of the human cervical spine under flexion and tensile loading conditions has recently been provided through human pediatric cadaver research (Ouyang, Zhu, Zhao, Xu, Chen, & Zhong, 2005). It follows that this new invaluable information on the biomechanical response and tolerance of the pediatric cervical spine be compared to that of the Hybrid III three-year-old child finite element model and if warranted, be incorporated in the child models design to improve its biofidelity and usefulness as a research tool. With more life-like child surrogates, researchers will be better able to evaluate the efficacy of child restraint systems and other interventions to mitigate the risk of injury and death.

1.2 Operating Definitions

Dummy: refers to the Hybrid III three-year-old child anthropometric test device.

Model: refers to the Hybrid III three-year-old finite element model.

Injury Protection Reference Values: the lower threshold for which an injury is likely to occur. Applies to dummies.

Injury Criteria: an assessment of the probability of a known acceleration, force or moment to cause injury. Applies to humans.

Global Coordinate System: denoted as X, Y and Z, and defined by the right-handed cartesian coordinate system convention.

Local Coordinate System: the coordinates are referenced to the centre of mass of the head and chest of the model and defined as positive x , being forward, positive y , originating from the models left shoulder and directed toward the right shoulder, and positive z , defined by the right-handed cartesian coordinate system convention.

1.3 Hypotheses

Hypothesis 1 - The neck of the Hybrid III three-year-old child finite element model is significantly stiffer than that of the pediatric cadaver cervical spine data.

Hypothesis 2 - The Hybrid III three-year-old child finite element model does not adequately predict the failure tolerance of the pediatric cadaver cervical spine data under axial tensile loading conditions.

Hypothesis 3 - The Hybrid III three-year-old child finite element model does not exhibit the same kinematic response of the pediatric cervical spine data under flexion loading conditions.

Null Hypothesis – There will be no difference in stiffness, failure tolerance or kinematic response under flexion between the neck of the Hybrid III three-year-old child finite element model and that of the pediatric cadaver cervical spine data.

2. LITERATURE REVIEW

2.1 Automotive Crash Statistics

2.1.1 Canada

Unintentional injury is the leading cause of death for persons between the ages of 1 through 34 years of age in Canada (Public Health Agency of Canada, 2006). The majority of unintentional fatal injuries (60.9 percent) are attributed to motor vehicle accidents (Public Health Agency of Canada, 1996). Statistics from Health Canada (2003) confirm that motor vehicle accidents account for the greatest number of child fatalities in Canada. In the year 2000 alone, there were 32 deaths and 3,148 injuries attributed to motor vehicle accidents for children aged 0 through 4 years of age in Canada (Statistics Canada, 2003).

2.1.2 United States

Similar statistical data reported by NHTSA (2002) confirms that motor vehicle accidents are the leading cause of child mortality in the United States. Statistics from the year 2004 indicate that every day, an average of 7 children between the ages of 1 through 13 were killed, and 800 more injured in motor vehicle accidents. In addition, in the same year, 9,078 child motor vehicle occupants were involved in fatal motor vehicle accidents (NHTSA, 2006). Further, the National Centre for Statistics and Analysis (NCSA) determined that in the year 2002, motor vehicle accidents accounted for 607 deaths and 62,000 injuries to children aged 0 through 5 years (NHTSA, 2006). It is evident from these statistics that motor vehicle accidents present a significant risk of injury and death for children in both Canada and the United States.

2.2 Injury

2.2.1 Patterns of Injury

Clinical observations documented from the Crash Injury Research Engineering Network (CIREN) calculated that motor vehicle accidents account for 50 percent of all pediatric trauma and 30-40 percent of pediatric cervical spine injuries (Brown, Brunn & Garcia, 2001; Kokoska, Leller, Rallo, & Weber, 2001; Patel, Tepas, Mollitt, Pieper, 2001; Brown, Ping, Wang, & Ehrlich, 2006). Approximately 50 percent of injuries to the pediatric cervical spine sustained in motor vehicle collisions (MVC's) are fatal (Patel et al., 2001). For children under 11 years of age, motor vehicle accidents account for 38 percent of all cervical spine injuries (McGrory, Klassen, & Chao, 1993). Paravertebral soft tissue injuries are the most common type of injury to the cervical spine, accounting for 68 percent of all spinal injuries. The most common spinal injury level was the high cervical spine, the occiput through the fourth cervical vertebrae (Cirak, Ziegfeld, Knight, Chang, Avellino & Paidas, 2004). More specifically, injuries of the Occipitoatlantoaxial (Occ-C2) complex (also known as atlanto-occipital injuries) are the most common form of cervical spine injury in children aged 10 years and younger (Sochor, Faust, Garton & Wang, 2004). Approximately 80 percent of all cervical spine injuries in children occur at levels above C2. In contrast, 84 percent off all cervical spine injuries to adults occur in the C3-C7 region (Dai, Ni, & Yuan, 1999; Hause, Hoshiro, & Omata, 1974). Traumatic cervical spine injuries to children include atlanto-occipital dislocations, fractures to the odontoid process and spinal cord lesions (Steinmetz, Lechner, & Anderson, 2003; Cirak, et al., 2004; Mousny, Saint-Martin, Danse, & Rombouts, 2001).

2.2.2 Case Studies

Due to the prevalence of cervical spine injuries in children involved in motor vehicle collisions, the primary area of improvement in the Hybrid III ATD over its predecessor (the Hybrid II) was neck biofidelity and response. Several investigators have previously studied ATD neck biofidelity by comparison of case studies of real world motor vehicles accidents and experimental crash tests (Howard, McKeag, Rothman, Mills, Blazeski, Chapman & Hale, 2005; Yannaccone et al., 2005; Sochor et al., 2004). The goal of the research is to identify real world motor vehicle accidents in which the following criteria are met; the child occupant(s) approximate the size and mass of the Hybrid III three-year-old ATD, injuries sustained in the crashes are well documented, and delta velocity (v) of the accident are known. Cervical spine injuries resulting from the accident are then compared to experimental crash tests run with the Hybrid III ATD under simulated crash conditions. Results are compared to determine if there is a difference in the ATD predicted injury verses the actual injury sustained. This has enabled researchers to validate ATD response and biofidelity.

A case study of interest is one in which three children ages 3, 6 and 7 were involved in a frontal motor vehicle crash. The MVC involved a 1994 Sport Utility Vehicle (SUV) which collided with a 1995 mid-sized sedan. The sedan had lost control on a wet road and presented it's passenger side to the case vehicle.

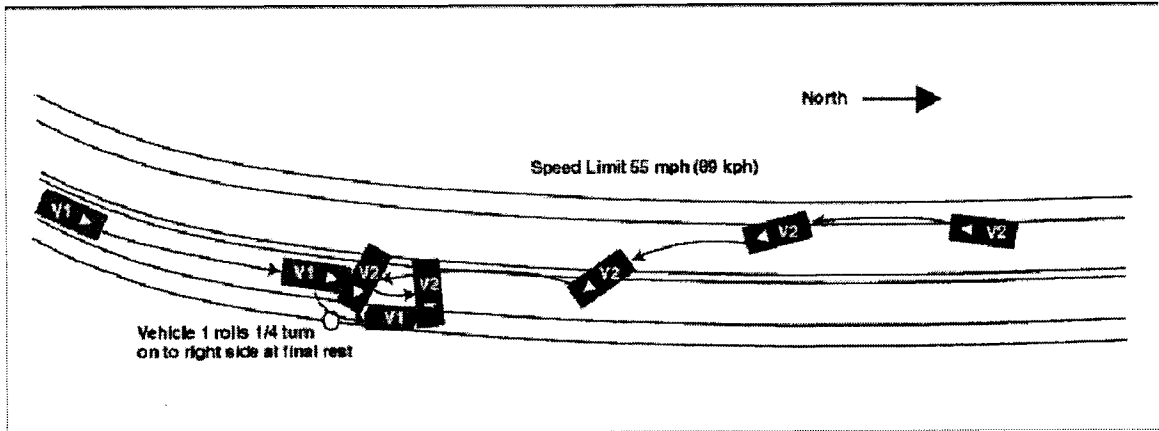


Figure 1. Accident reconstruction diagram (Sochor et al., 2004).

The delta v of the crash was approximately 45 km/h.



Figure 2. Case vehicle, a 1994 SUV (Sochor et al., 2004).

The child occupants were restrained with only a lap belt and all survived the crash. All three children had varying degrees of Occ-C2 injury without permanent neurological

damage leading the researchers to believe that the children were at the lower threshold of serious neck injury. Similar research previously conducted by Mertz, Driscoll, Lenox, Nyquist & Weber (1982) on porcine subjects established the presence of an AIS 3 (serious) injury based upon the presence of hemorrhage in the synovial fluid of the occipital condylar joint capsule. All three child occupants had varying degrees of hemorrhagic rupture in the vicinity of the ligaments which encase the occipital condylar joint. It was concluded by Sochor et al., (2004) that all three children experienced loading close to their individual neck tolerance limits.

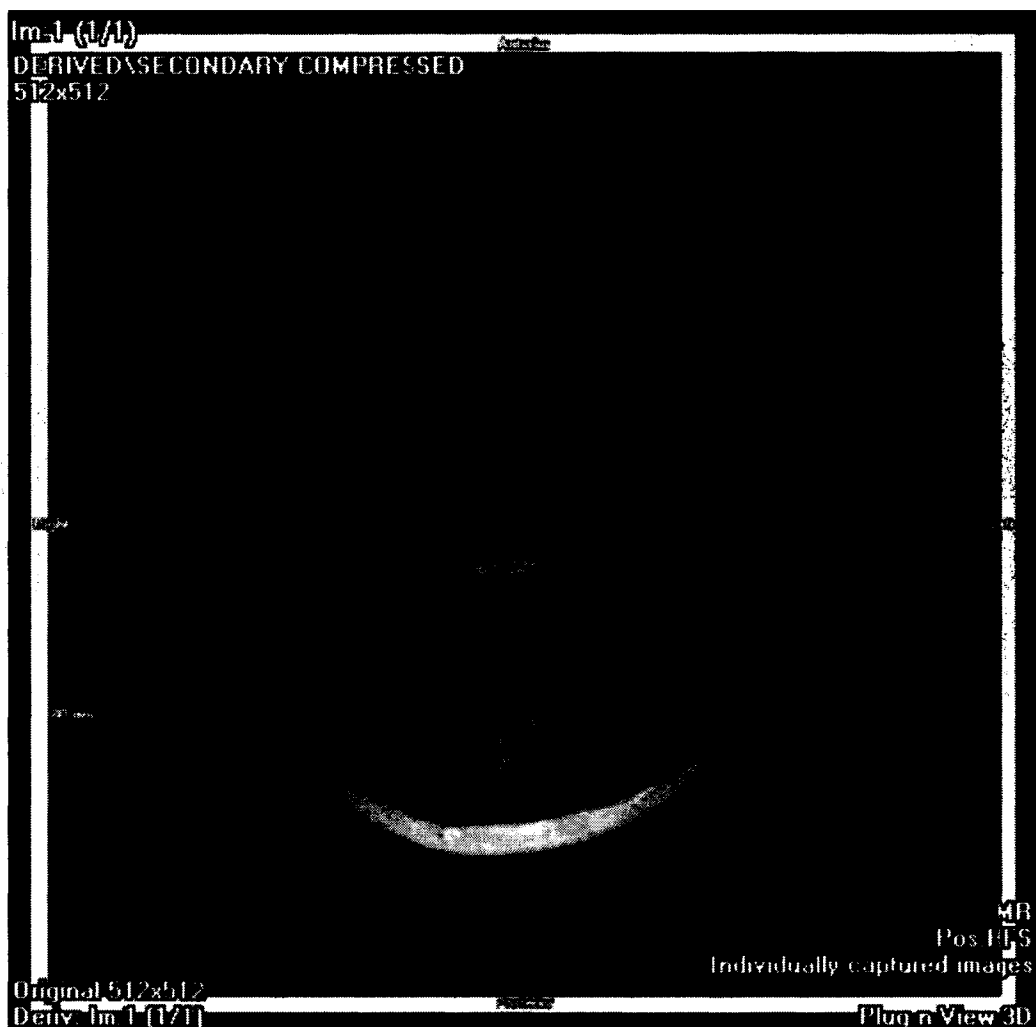


Figure 3. Slight hemorrhage at the tectorial membrane (Sochor et al., 2004).

Sochor et al., (2004) reconstructed the crash using MADYMO computer modeling simulation software. The SUV/Hybrid III ATD model was run on the deceleration pulse specified in the Federal Motor Vehicle Safety Standard (FMVSS) 208 (125 ms 48 km/h sled pulse) which was close to the delta v for the MVC. The modeled neck loads were near the neck injury criteria specified by the FMVSS 208 for 3 and 6 year-old ATD's. Non-contact NIJ values peaked prior to significant head rotation and peak neck tension. The model injury criteria predicted a 3-5 percent risk of an AIS 3 injury. The injury assessment reference values (IARV) of the model correlate well with the actual AIS 2 (moderate) injuries the children sustained in the MVC indicating that the IARV appear to be appropriately set. The study conducted by Sochor et al. (2004) is limited by the fact that analysis was based on only one acceleration pulse of moderate intensity. The full range of acceleration intensity from minor to failure was not considered. Due to the viscoelastic response of human tissue to loading, the response and correlation to other acceleration pulses are unknown.

Several other case studies support a non-contact mechanism of injury. Howard et al., (2005) analyzed a case study in which a 23 month-old-child was properly restrained in a forward facing CRS and was involved in a MVC with a delta v of 40 km/h. The child suffered a fatal Occ-C1 dislocation. In a second case, a 35 month-old-child who was properly restrained in a forward-facing CRS was involved in a MVC with a delta v of 80 km/h and suffered a fracture to C2. The child recovered from the injury. Further analysis by Howard et al. (2005) of 5,000 MVC's from the National Automotive Sampling System Crashworthiness Data System revealed that adult occupants seated in the front seat sustained less severe injuries than child occupants in CRS's seated in rear seats. In

all cases, the children were the furthest occupants from the point of impact, yet received the more serious of injuries. It is thus evident that children are at an increased risk of injury in MVC's as compared to adults. Researchers have cited the fragile pediatric cervical physiology as a mechanism for increased injury (Weber, 1995).

2.3 Injury Mechanism and Biomechanics

2.3.1 CRS as a Mechanism to Reduce Injury

Forward facing CRS's reduce the risk of serious injury and hospitalization by 78 percent for children 1 through 4 years of age involved in a MVC as compared to children restrained only by a seat belt. The biomechanical principal of a CRS is to distribute the crash forces over the shoulders and hips, as well as to control head excursion during the crash event (Arbogast, Durbin, Cornejo, Kallan, & Winston, 2004). CRS's that are secured to the vehicle by Lower Anchors and Tethers for Children (LATCH), and Top Tethers, rigidly couple the CRS to the vehicle body allowing the CRS and child occupant to effectively "ride-down" the rapidly changing velocity of the crash. Coupling the CRS to the vehicle body allows the deceleration pulse of the MVC to be coupled with the energy absorbing crumple zones on the vehicle. This dissipates the energy of the crash over a longer period of time thereby reducing the impact forces on the occupant (Arbogast et al., 2002). This research concludes that attenuating the rate of change of velocity a child experiences in a MVC reduces their risk of injury.

2.3.2 Velocity and Time Duration as Injury Mechanisms

Nance, Elliott, Arbogast, Winston, & Durbin (2006) examined the association between delta v and risk of injury to children involved in frontal motor vehicle crashes. Nance et al., defined delta v as the difference in initial v at the instant prior to impact and

the final v , assumed to be zero, for the MVC. The probability of an AIS 2 injury increased on average 56 percent for each 10 kph increase in Δv . The Δv at which 50 percent of child occupants would be expected to sustain an AIS 2 injury was 37 kph and that of an AIS 3 injury was 63 kph. The researchers concluded that Δv is strongly positively correlated with and predictive of injury risk for child occupants.

Research done by Desantis-Klinich, Saul, Auguste, Backaitis, & Kleinberger (1996) found an inversely proportional relationship between the duration of time a load was applied for and the critical load to cause injury. As the time duration increases, the critical load to cause injury decreases. As an example, axial tensile neck loads of approximately 2,500 N imparted on the neck of a three-year-old can be sustained from 0 to approximately 20 ms. After 20 ms, the critical load that can be sustained is greatly reduced. For example, after 30 ms, the critical load that can be sustained without causing injury is approximately 1,000 N.

2.3.3 Pediatric Cervical Spine Anatomy

To fully understand the injury potential and effects on the pediatric cervical spine, we must first understand the anatomy of the spine. The occipital condyles are found at the posterior base of the skull and articulate with the atlas. The condyles are seated in concavities in the lateral mass of the atlas. These concavities develop with age and are absent in the pediatric cervical spine. A lax ligamentous capsule surrounds the atlantooccipital articulation and provides most of the stability of the occipital cervical junction. The most important ligaments for stability are the tectorial membrane, cruciate ligament and the alar and apical ligaments. Many of these ligaments are underdeveloped in children (Steinmetz et al., 2003). Anatomical and developmental differences between

the pediatric and adult cervical spine result in a greater mobility of the pediatric cervical spine due to greater ligamentous laxity, shallow angulations of the facet joints, immature development of the neck musculature and incomplete ossification of the vertebrae (Roche & Carty, 2001).

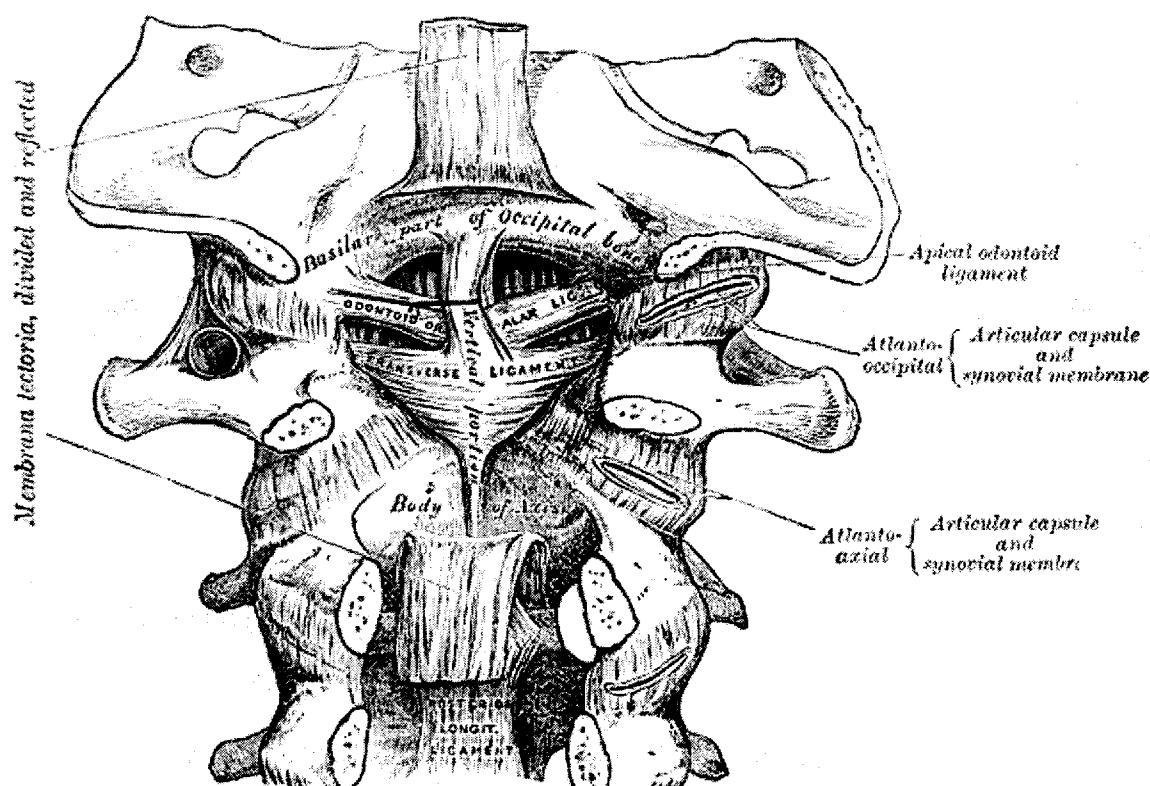


Figure 4. Posterior view of the Occ-C2 complex and tectorial membrane (Gray, 1860).

In addition, the comparative anatomy of the pediatric head lends to cervical spinal injury. This is due primarily to the relative size and mass of a child's head as compared to the rest of the body. The ratio of head to body mass is 1:3 for newborns and 1:15 for adults. Therefore, the mass of a child's head is proportionately greater than that of an adult (Cassan, Caillieret, & Tarriere, 1992). The greater mass of the pediatric head along with the reduced structural integrity of the pediatric neck lend to cervical spine injuries in MVC's.

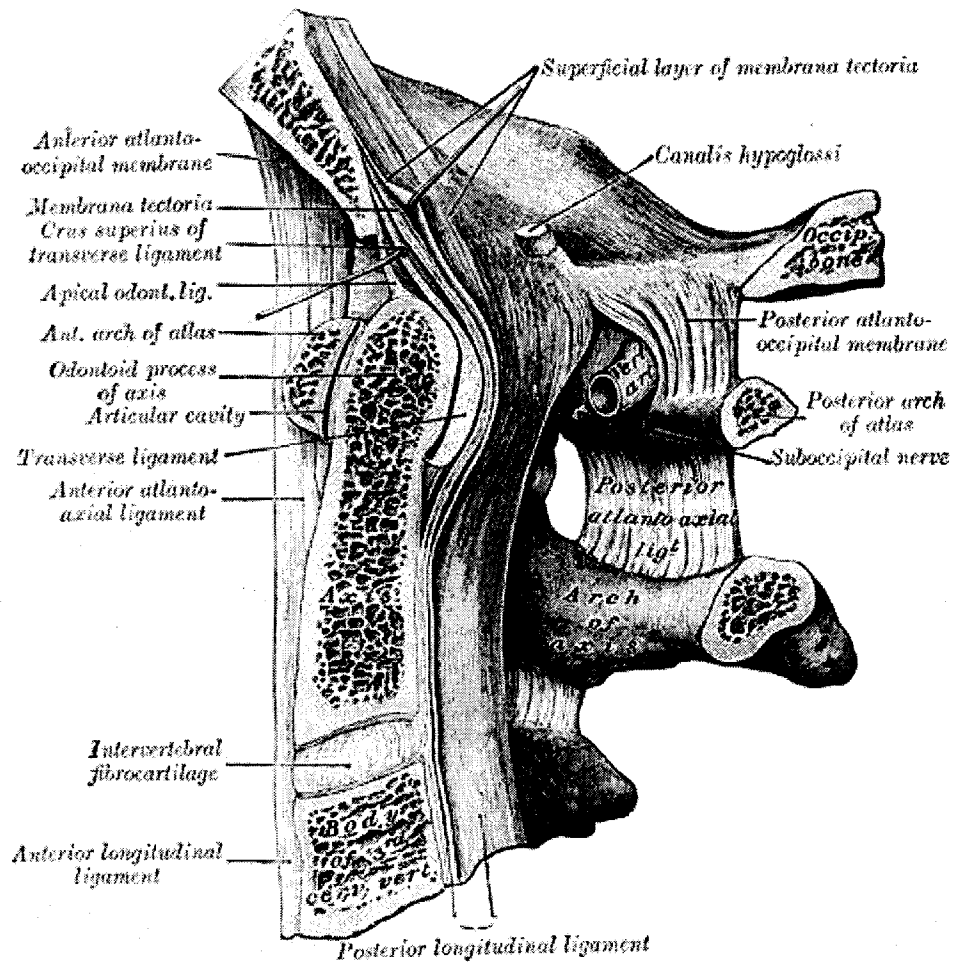


Figure 5. Medial sagittal plane of the Occ-C2 complex (Gray, 1860).

2.3.4 Biomechanics of the Pediatric Cervical Spine

The relative biomechanical contribution of the Occ-C2 complex to flexion and axial distraction of the human spine can be summarized as follows. The atlantooccipital complex contributes to 25 degrees of flexion-extension, 5 degrees of lateral bending and 5 degrees of rotation (Anderson, 1988; Anderson & Montesano, 1992; Bools & Rose 1986). Extension is limited by the tectorial membrane and flexion is limited by contact of the dens and the basion. Lateral bending is counteracted by the alar ligaments. Distraction is opposed by the tectorial membrane and the alar ligaments.

The biomechanical structure and biomaterial properties of the pediatric cervical spine place children at an increased risk of acceleration induced injury as experienced in MVC's (Huelke, Mackay, Morris, & Bradford, 1991; Myers & Winkelstein, 1995; Weber, 2002; Yoganandan & Kumaresan, 2002). The ligaments of the pediatric cervical spine are lax and do not effectively contribute to the structural integrity of the cervical column. The cervical vertebrae are not yet completely ossified making them more prone to separation. The facets are predominately horizontal which provide little restriction to dislocation and the posterior-lateral contours of the vertebral bodies are not developed and therefore can not restrict flexion-rotation forces (Fuchs, Barthel, Flannery, & Christoffel, 1989; Janssen, Nieboer, Verschut, & Huijskens, 1991; Weber, 2002; Yoganandan et al., 2002). In addition, the relatively large head and shorter neck of children places the fulcrum of the cervical spine within the Occ-C2 complex increasing the risk for Occ-C2 dislocation injuries (Steinmetz et al., 2003). As a result of these biomechanical factors, 60-80 percent of all pediatric vertebral injuries are in the cervical region.

2.3.5 Resultant Mechanism of Injury and AOD

Anatomical, physiological and developmental differences between children and adults place children at an increased risk of head and neck injury as compared to adults. Mechanisms of neck injury include extreme hyperflexion which leads to rupture of the tectorial membrane and separation of vertebrae which leads to atlantooccipital dislocation (AOD) (Dublin, Marks, & Weinstock, 1980). Separation occurs in the immature pediatric cervical spine due to the column not yet having formed a contiguous interlocking structure through the normal processes of growth and development such as ossification

and geometric changes. This structural inadequacy in high axial tension-forward flexion environments as experienced in MVC's damages the spinal cord by placing it in a state of tension or complete transaction (Arbogast et al., 2002). The disproportionate size of the child's head relative to the rest of the body increases the relative moment of inertia per unit of acceleration for children as compared to adults. This in combination with the under developed musculoskeletal pediatric cervical spine put children at an increased risk for cervical injuries in MVC's.

The combination of tension and forward flexion in and of itself is an injury mechanism for Occ-C2 dislocation injuries. Research conducted on primates has determined the tolerance of the cervical spine to Occ-C2 dislocation injuries is estimated to occur at approximately 120 g's (Thomas & Jessop 1983). Occ-C2 dislocations occur more frequently in children due to their relatively small occipital condyles, ligamentous laxity and flat articulation between the occiput and the atlas.

2.4 Head and Neck Injury

2.4.1 Head Injury

Approximately 19 percent of children involved in MVC's sustain injuries to the head. Head injuries include both contact and non-contact injuries and are primarily induced from acceleration forces. Contact injuries include skull fracture, epidural hematoma and frontal lobe contusion and are the result of head excursion and impact with the vehicle interior (Gennarelli, 1986, 1993). The primary concern of head injury is injury to the brain caused by acceleration induced contusions to the cerebral cortex.

The major concern in head injury is injury to the brain. The major mechanisms of brain injury are positive pressure, negative pressure and shear due to pressure gradients.

When the head is impacted, positive pressure is developed as a result of compressive stress. Similarly, at the site opposite to the location of injury, negative pressure develops due to tensile loading. Injuries to the brain due to motion of the brain relative to the skull result in contusions on the surface of the brain which are attributed to shear caused by pressure gradients. Shear injuries are often the result of large angular accelerations of the head (King, 2000).

Research conducted at Wayne State University has developed the Wayne State Tolerance Curve (WSTC) for linear head acceleration. The curve shows that the brain is able to tolerate higher accelerations if the acceleration pulse is shorter in duration. Gadd (1966) advanced the WSTC by approximating a straight line with a slope of -2.5 would fit the data when plotted on a logarithmic scale. This curve became known as the Gadd Severity Index (GSI). Versace (1971) furthered the work of Wayne State and Gadd by modifying the WSTC and GSI to the Head Injury Criterion (HIC) which has been adopted by the FMVSS 208.

$$HIC_{t_2-t_1} = \left(\frac{1}{t_2-t_1} \cdot \int_{t_1}^{t_2} a_g \cdot dt \right)^{2.5} \cdot (t_2-t_1)$$

Where:

a is the resultant acceleration of the centre of gravity of the head (g) and numerically is equal to the sum of the squares of the local x , y and z components of acceleration.

$$a_{resul\ tan\ t} = \sqrt{a_x^2 + a_y^2 + a_z^2}$$

t_1 , t_2 are points in time of interest during the crash event (s)

The HIC measures the effects of head acceleration and duration. These parameters are easily measured by accelerometers on ATD's. The criteria is valid for linear acceleration

impacts. In most MVC's, both linear and angular acceleration are present, however, due to lack of another acceptable measure, the criteria is accepted by researchers and government regulatory agencies in frontal crash vehicle compliance testing.

2.4.2 Neck Injury

It has been shown that neck injury is an obvious concern for children involved in MVC's. The Normalized Neck Injury Criterion (Nij) is used in experimental testing to predict the injury potential in frontal impact crashes. The Nij is simply the sum of the forward rotational moment and the axial tensile load for the cervical spine. Both are normalized to a critical value and are ATD specific. ATD's are fitted with accelerometers that measure the rotational moment and load cells that measure axial tension. Unlike the HIC, and due to lack of knowledge on pediatric cervical spine trauma, NHTSA decided not to incorporate the NIC into FMVSS and suggested further research into this area is required.

Recent research conducted by Yannaccone et al., (2005), compared the dynamic response of the Hybrid III three-year-old ATD in an experimental crash to a real-world crash in which the child occupants sustained serious cervical injuries. A neck injury assessment was calculated based on the data from the ATD using the Nij (NHTSA version 10). Nij combines the flexion-extension moment with the tension/compression axial force while making a correction for the offset of the moment axis in the load cell from the occipital condyle. The Nij makes no such correction for the moment arm for the occipital condyle.

$$N_{ij} = \left(\frac{F_z}{F_{zc}} \right) + \left(\frac{M_y + (OC \cdot F_x)}{M_{yc}} \right)$$

Where:

F_z is axial force

F_{zc} is critical values for axial force

M_y is the fore/aft moment

M_{yc} is critical values for fore/aft moment

OC is occipital condyle offset

F_x is fore/aft shear force

The study revealed that children exhibit a greater degree of flexibility in the lumbar and thoracic spine which is consistent with previous findings by Cassan, Page, Pincemaille Kallieris, & Tarriere (1993) in a study comparing child cadavers to ATD's. The researchers also suggested that the lack of bending in the torso may increase the extension of the upper neck as similarly reported by Sherwood et al., (2003) with the Hybrid III six-year-old ATD. The results of the current study suggest that the kinematics and dynamic response of the experimental tests appear relatively consistent with the injuries sustained by the children in real world crash events. Inconsistencies with previous studies (Hendersen, Brown, & Paine, 1994) suggest that the current Nij reference value may be too conservative or the neck of the Hybrid III three-year-old ATD is not sufficiently biofidelic, particularly, in the rotational flexibility of the Occ-C1 joint. The findings of Hendersen et al., are consistent with findings of other researchers on the neck of the Hybrid III six-year-old, concluding the stiffness of the Hybrid III may be inducing high neck forces and moments that are not indicative of the true injury potential (Sherwood et al., 2003; Mallot, Arbogast, Cooper, Murad, Ridella, Barnes, Kallan, & Winston 2003; Menon, Cooper, Murad, Ridella, Barnes, Kallan, & Winston 2003).

2.4.3 Chest Injury

The Combined Thoracic Index (CTI) is an injury criterion used for the chest in case of frontal impacts. The CTI is evaluated using the peak average 3 ms value for resultant acceleration of the spinal cord and chest deflection.

$$CTI = \left(\frac{A_{\max}}{A_{\text{int}}} \right) + \left(\frac{D_{\max}}{D_{\text{int}}} \right)$$

Where:

A_{\max} = 3 ms value (single peak) of the resultant acceleration of the spinal cord (g)

A_{int} = Critical 3 ms value (g)

D_{\max} = Deflection of the chest (mm)

D_{int} = Critical deflection (mm)

Note: A_{int} and D_{int} for the Hybrid III three-year-old are 70 g and 57 mm respectively.

2.5 Overview of Testing Methodologies Applicable to the Problem

2.5.1 Experimental

Experimental testing on the response and tolerance of human tissue under dynamic loading conditions is difficult, due to obvious moral and ethical issues. Research must be conducted on adult volunteer subjects and limited to sub injurious levels. While this type of live volunteer testing may be useful in determining the lower threshold of discomfort or pain, the data can not easily be extrapolated to draw conclusions for injurious levels or predict child injury potential and tolerance. Alternatives to this form of experimental testing include analysis of MVC case studies as described in previous sections, analysis of accidental free falls of children, cadaver studies and studies on isolated primate and adult human cadaver structures. The following provides an overview

of previous experimental studies conducted on the dynamic response and injury tolerance of the pediatric head and neck.

Early research conducted by Mohan Mohan, Bowman, Snyder, & Foust (1979) studied head impact injuries for children involved in accidental free falls. The study consisted of a summary of the data for 30 children aged 1 to 10 years who were involved in an accidental free fall for which the conditions were documented in medical reports. The study yielded initial estimates of pediatric tolerance limits for moderate head injuries (AIS 2). The tolerance was determined to be in the range of 200-250 g's for peak acceleration and 150-200 g's for a 3 ms average head acceleration. The researchers concluded that acceleration based measures are suitable as predictors of head injury severity.

Other preliminary research on pediatric response and tolerance to frontal MVC's was performed by Kallieris, Barz, Schmidt, Heess, & Mattern (1976). Experimental frontal crash tests were conducted with four child cadavers and one child ATD restrained in CRS's. Comparison of the kinematics of the child cadavers and child ATD revealed that the movement of the head, neck and shoulders were practically identical. The difference was in the response of the spinal column, the child ATD was stiffer in the thoracic and lumbar spinal regions. The child cadavers exhibited a greater degree of flexion, up to 90 degrees, in the thoracic and lumbar regions whereas the child ATD flexion reached a maximum of 25 degrees.

Cassan et al., (1993) later compared the kinematic and dynamic responses of child cadavers and child ATD's in experimental frontal vehicle crashes utilizing accelerometers and force transducers. Maximum axial tensile forces in the neck of 1570-

1600 N were recorded from the ATD. The cadaver subject sustained AIS 3 neck injuries consisting of a fracture to the dens axis and hemorrhages of the intervertebral disks. The maximum head acceleration on the ATD was found to be 116 g. There was no corresponding injury observed on the child cadaver subjected to identical experimental testing conditions. The sub injurious head acceleration of 116 g is consistent with the tolerance calculated by analysis of accidental child free fall.

There is a general paucity of child cadaver research on the response and tolerance to bending moments and axial loading. To compensate for this, researchers have utilized primates as human surrogates to study the effects of dynamic loading on the pediatric cervical spine. Nuckley, Hertsted, Eck, & Ching., (2005) studied the effect of the displacement rate on the tensile mechanics of pediatric baboon cervical spines. The tensile stiffness and failure load significantly increased with displacement rate. A two-fold increase in stiffness and a four-fold increase in failure load were observed when the displacement rate was changed from 0.5 mm/s to 5000 mm/s. The results of the study are consistent with other researchers (Yoganandan, Pintar, Maiman, Cusick, Sances, & Walsh, 1996; Van Ee, Nightingale, Camacho, Chancey, Knaub, Sun, & Myers, 2000; Ching, Nuckley, Hertsted, Mann, & Sun, 2001) who reported a three-fold increase in failure load. Utilizing the rate dependant mechanics of cervical spine tissue is important for accurate modeling of the spine under dynamic loading conditions.

Additionally, research performed on the adult female cervical spine provided a theory explaining the prevalence of upper cervical spine injury. Nightingale, Winkelstein, Knaub, Richardson, Luck, & Myers (2002) compared the strengths and structural properties of the adult female upper and lower cervical spine in flexion and extension. It

was concluded that the ligamentous upper cervical spine was significantly stronger than that of the lower cervical spine despite the prevalence to upper cervical spine injuries. Van Ee et al., (2000) attributed this discrepancy to the effects of active musculature. The muscles of the cervical spine share tensile loads with the ligaments. This load sharing increases the overall strength of the cervical spine. This effect is greater for the larger size and number of muscles in the lower cervical spine (Van Ee et al., 2000).

Further, research suggests that occipito-atlanto and atlanto-axial dislocation injuries may occur by identical loading mechanisms that result in two different structural failures along a common load path. In occipito-atlanto dislocation injuries, tensile stresses cause the alar ligaments and the superior cruciform ligament to fail. This results in rapid failure of the remaining ligaments. Atlanto-axial dislocation injury occurs when the same tensile stress causes an avulsion of the dens from the body of C2. The failed dens and the superior cruciform ligament cause C1 and the odontoid to separate from C2 (Nightingale et al., 2002). The likelihood of each failure mode is dependant on anatomical differences of the subject (Ryan & Henderson, 1992). This research identifies an important finding in the load sharing ability of skeletal muscle and highlights the limitations of experimental studies utilizing isolated cervical spines.

Despite the previously identified limitation, conducting experimental tests on cervical spines with intact skeletal muscle raises issues due to the variability that muscle mass, tone or activation will induce. Ouyang et al., (2005) performed a biomechanical assessment on isolated pediatric cervical spine complexes obtained from pediatric donors aged 2 through 12 years. The pediatric cervical spines were subjected to flexion-extension bending and tensile loading tests to characterize their biomechanical response and

tolerance. With the exception of a study completed in the 1874 by Duncan, there have been no other documented cadaver studies on the tolerance of the pediatric cervical spine. Ouyang et al., (2005) found the average rotational Occ-C2 stiffness to be 0.72 and Occ-T2 0.04 N·m /degree. Tensile failure occurred for the 2 through 4 year-old specimens at average distraction force of 595 N. Duncan found the average cervical tensile failure load for a sample of 4 stillborn infants to be 470.5 N. The average linear stiffness in tensile loading was 34.7 N/mm. Both average rotational stiffness and average tensile stiffness were independent of pediatric age (Ouyang et al., 2005).

2.5.2 Theoretical

Theoretical forms of testing employ the application of physical laws of motion and contact to a hypothetical impact or crash. Principals of Newtonian physics like impulse-momentum may be used to formulate free body diagrams and estimate accelerations or loads. The lumped mass model is an example of a theoretic model and has been shown to correlate with human cadaver testing. The model consists of rigid body elements assigned a mass connected by spring and damper elements. The mass elements represent body structures, such as bone, and the spring and damper elements represent the soft tissue (Wismans, 2004). The limitation of theoretical models, such as the lumped mass model, emphasizes the fact that vehicle crashworthiness and the mechanical response of human tissue is a complex problem. The theoretical approach to modeling does not adequately allow for the quantification of non linear phenomenon such as contact, material properties or geometry.

2.5.3 Numerical

Recent technological advancements in computer processor speeds enabled the use of numerical methods such as finite element analysis which has proved to be an invaluable tool in vehicle crashworthiness and occupant protection research. Finite element analysis, simply put, is an approximation to governing equations of inertia, viscosity and dampening, which defines the material properties of matter. Finite element analysis software performs the simultaneous solution of coupled second order differential equations. These equations define the material properties of each finite element of the model. The inputs to the model are approximations to acceleration, velocity and displacement. A more detailed explanation of finite element analysis and modeling is presented in the appendices.

The advantage of finite element analysis over other numerical methods is the ability to predict local structural deformations and stresses. The disadvantages of the finite element method include the time required to create a representative model with accurate and correct geometry, limited material property data for biological tissues and computation time for complex simulations may be on the magnitude of several days.

Dupuis, Meyer, & Willinger (2005) attempted to resolve the issue of model geometry by using a medical scanner to image the cervical spine of a three-year-old child. The image geometry was compared to that of an existing adult model and remeshed to create a finite element model of the pediatric cervical spine. The model included the anatomical structures of the head, C1 through C7, the first thoracic vertebrae (T1), the intervertebral disks and the principal ligaments. The intervertebral disks were scaled from data obtained from Yoganandan, Pintar, Kumaresan, & Gennarelli (2000)

and the material properties for the ligaments from complimentary research done by Myklebust, Pintar, Yoganandan, Cusick, Maiman, Myers & Sances (1988), Chazal, Tanguy, Bourges, Gaurel, Escande, Guillot, & Vanneuville (1985) and Yoganandan et al., (2000). The response of the model was tuned to fit the results of experimental frontal and rearward impact test of the head and neck of a Q3 ATD. The limitations of the study lie in the inherent problem of validating the finite element model to the response of a child ATD, as opposed to actual human tissue response.

Other researchers have used finite element modeling and have established an acceptable correlation between numerical simulations and experimental crash tests. Turchi, Altenhof, Kapoor, & Howard (2004) compared the head and chest accelerations of experimental crash tests and numerical simulations. In the experimental tests, the Hybrid III three-year-old dummy was positioned in a CRS in accordance with FMVSS 213 in a five point harness. The CRS was attached to the test apparatus via the LATCH system. The numerical model of the Hybrid III three-year-old dummy was provided by First Technology Safety Systems (FTSS). The dummy model was positioned in a finite element model of a CRS provided by the Graco Corporation. The child dummy/CRS model was loaded under FMVSS 213 conditions.

Validation of the numerical model was completed by a comparison of the experimental test data and the numerical simulation data. The head and chest acceleration data verses time were plotted and compared and it was observed that an acceptable correlation existed. The head and chest acceleration profiles were similar. The local x and z head acceleration occurred when the head reached the greatest degree of flexion rotation for both the numerical and experimental tests.

Kapoor, Altenhof, & Howard, (2005) used the finite element model of the Hybrid III three-year old child dummy and CRS to investigate the effect of CRS anchorage method on the injury potential for children in frontal crash. The sensitivity of the numerical model was sufficient in determining the difference in anchorage method. Further numerical model validation was completed by Kapoor, Altenhof, Wang, & Howard. (2006). Similar to Turchi et al., (2004), experimental test data was compared to numerical simulation data, however, in addition to head and chest acceleration data, neck force and moment data were incorporated into the research design. Experimental crash tests were conducted by Transport Canada with the Hybrid III three-year old child dummy positioned in a CRS in a 2004 Mitsubishi Lancer in accordance with CMVSS 208. The numerical model of the Hybrid III three-year-old child and CRS were prescribed an acceleration pulse consistent with that of the experimental test.

Turchi et al., (2004) concluded similar local x and z head accelerations components were observed for the experimental and numerical dummies. The time to peak local x head acceleration was similar with the maximum local x and z head acceleration being a minimum at maximum head flexion. Kapoor et al., (2006) found the upper and lower neck forces exhibited similar time profiles. Higher magnitudes of neck forces were found in the upper neck load cell as compared to the lower neck load cell. This finding is consistent with research done by Sances et al., (2002) who found that the upper neck and head transmits approximately 75 percent of forces to the lower neck. Both dummies exhibited similar time profiles for upper and lower neck moments. The neck moments were higher for both dummies in the lower neck region. Head and neck injury criteria were calculated for the experimental and numerical dummies. The

maximum percentage error between experimental peak values and numerical predictions was calculated to be no more than 15 percent.

3. FOCUS OF RESEARCH

The current state-of-the-art Hybrid III three-year-old child dummy and model are used by governments and industry in experimental vehicle frontal crash tests to evaluate the effect of varying vehicle or safety equipment design on the injury potential of child occupants. The Hybrid III utilizes a braided steel cable to model the response of the human pediatric cervical spine under bending and tensile loading conditions. The literature review has shown that previous researchers have found the response of the Hybrid III dummy to overstate the stiffness of the human cervical spine under compression loading conditions. No research has made comparisons to stiffness of the Hybrid III dummy neck under axial tensile or flexion loading conditions. Moreover, no research has attempted to compare the response of the Hybrid III three-year old child finite element model under axial tensile or flexion loading conditions to pediatric cervical spine cadaver data. In addition, precise failure tolerances for the neck of the Hybrid III dummy and model are lacking and attempts to incorporate the material properties of the human cervical spine obtained from pediatric cadaver research into the Hybrid III three-year old finite element model have not yet been made.

The focus of this research is specifically to:

- 1) Determine if there is a difference for the stiffness of the neck of the Hybrid III three-year-old child finite element model and human pediatric cadaver cervical spine specimens.
- 2) If a difference exists, incorporate an axial tensile load failure tolerance curve for the pediatric cervical spine in the Hybrid III three-year-old finite element model.

- 3) Improve the response of the neck of the Hybrid III three-year-old finite element model when subjected to flexion and tensile loading to enable the model to better predict peak neck loads and moments.
- 4) Thus improve the biofidelity of the neck of the Hybrid III three-year-old child finite element model thereby increasing its efficacy as a research tool.

Such a contribution to knowledge will allow researchers to better predict the effect of vehicle safety equipment design iterations on the injury potential of children in motor vehicle accidents.

3.1 Limitations of the Proposed Study

Due to the lack of available pediatric cadaver research, this study is based on data obtained from a small sample of 5 pediatric cadaver cervical spine donor's biomechanical responses to bending and tensile loading. The small sample size is not representative of response variability of the entire population. It is also possible that damage to the pediatric cervical spines occurred during their disarticulation from whole body tissue or during the preceding non destructive tests. A limitation of using human cadaver data is the problem of applying human data to anthropometric test devices. It is probable that this study will be limited in that the contribution of cervical spine skeletal muscle to the tensile response is lacking due to removal of such tissues during the specimen preparation. Skeletal muscle shares the tensile load with the ligaments of the cervical spine providing a parallel load path. Such load sharing increases the overall strength and stability of the cervical spine (Van Ee et al., 2000). In addition, this study is only applicable to the response under flexion and axial tension loading conditions, extension and axial compression will not be considered. This study is also only applicable to the

Hybrid III ATD model and not other models such as the THUMS. Lastly, the displacement rate and dynamic characteristics of the material is similar to quasi static state in that the velocities are less than 10 m/s. Despite these limitations, the author is confident that the data used in this experimental procedure is both reliable and valid.

4. EXPERIMENTAL PROCEDURE OR METHODS

4.1 Experimental Procedure

The experimental procedure to determine the biomechanical response of the pediatric cervical spine under bending and tensile loading was conducted by Ouyang et al., (2005). Briefly, cervical head and neck complexes were obtained from pediatric donors aged 2 through 12 years of age. Neck musculature was removed and the cervical spines were subjected to quasi-static tensile load tests. A pure tensile load was applied by the test apparatus that allowed for full anterior-posterior translation and flexion-extension rotational degrees for freedom. The head-neck complex was subjected to a destructive test in which the displacement was increased at a rate of 5 mm/s until a 10 percent reduction in axial tensile load was observed. Axial tensile force data was collected via a load cell at the base of T2. The average linear stiffness for tensile loading was calculated to be 34.7 N/mm with no statistically significant difference found for pediatric age.

For the purposes of this project, data from a subset of 5 of the original 10 subjects studied by Ouyang et al., (2005) was used. The age range for the subset of subjects was 2 through 5 years of age. The force-displacement data from the five subjects has been provided by Ouyang et al., (2005) and was cross plotted using Mathcad 13 (Parametric Technology, Needham, MA). A cubic spline interpolation was performed for each subject to produce a polynomial function with continuous values for derivatives of displacement. The 5 curves can then be fitted and averaged to produce an average load-deflection curve for the 5 subjects of interest and subsequent calculation of the linear tensile stiffness (k). The slope of the resultant load-deflection curve is the stiffness (N/mm).

4.2 Numerical Procedures

A comprehensive explanation of the finite element method (FEM) is beyond the scope of this thesis. An overview of the finite element method is provided in appendix A. Validation of the Hybrid III three-year-old finite element model has been completed by previous research which established an acceptable correlation between the mechanical response of the Hybrid III three-year-old child dummy and the Hybrid III three-year-old child finite element model (Turchi et al., 2004; Kapoor et al., 2006). The results of these studies were presented previously in section 2.5.3 of this manuscript.

4.2.1 Preparation of the Finite Element Model Head-Neck Complex

For the initial part of this study the hypothesis that the neck of the Hybrid III three-year-old finite element model is stiffer than that of the pediatric cadaver cervical spine was tested. A finite element head-neck complex was obtained by disarticulating the Hybrid III model at the adapter plate just caudal to C7. By importing the Hybrid III model obtained from FTSS into the finite element model builder (FEMB), all superfluous parts were removed. In addition, material properties of the cervical vertebrae will be assigned a null material property to ensure they did not contribute to axial tensile forces. The intent of this research was to measure the response of the braided steel neck cable to tensile loading as compared to that of the pediatric cervical spine. In addition, single point constraints (SPC) were applied to the C7 to prevent translation when the tensile load was applied to the top of the model head.

Once complete, the FE head-neck complex can then be exported and numerical simulations completed using the explicit finite element code LS-DYNA version 970 revision number 5434a (Livermore Software Technology Corporation, Livermore, CA)

on a personal computer with a single 1.86 GHz Intel Pentium processor with 512 MB of random access memory. A displacement rate of 50 mm/s was applied to a node on the top of the head to mimic the time duration loading experienced in a MVC. It is important to note that a similar displacement rate as used by Ouyang et al., (2005) is not required as the braided steel cable for the rates of loading will not exhibit any rate dependence (Jones, 1989).

To test the hypothesis that the neck of the Hybrid III three-year-old child finite element model does not adequately predict the failure tolerance of the pediatric cadaver cervical spine data, the maximum tensile load of the model prior to failure was compared to that of the pediatric data at a similar instant. To test the hypothesis that the Hybrid III three-year-old child finite element model does not exhibit the same kinematic response of the pediatric cervical spine data under flexion loading conditions, the material properties of the pediatric cervical spine data was applied to the braided steel neck cable.

4.2.2 Extraction of Data from the Hybrid III Finite Element Model

Head acceleration data was acquired through kinematic observation of nodes located at the centre of gravity of the head of the Hybrid III model that represent accelerometers. The nodes acquire acceleration data in the local x , y and z directions. Acceleration data was filtered in accordance with the Society of Automotive Engineers (SAE) J211 class 1,000 second order Butterworth filter.

Upper and lower neck forces and moment data were acquired via finite element upper and lower neck load cells located in the upper and lower neck at locations that approximate the location of the load cells in the child dummy. Zero length beam elements modeled using material type 66 (linear elastic discrete beam) act as stiff translational and

rotational springs. Data were filtered in accordance to SAE J211 class 1,000 and 600 filters for the neck force and moment respectively.

Chest deflection will be measured by the relative displacement of two nodes in the chest region of the Hybrid III model that approximate the location of the chest deflection potentiometer in the child dummy.

4.2.3 Incorporation of the Pediatric Data into the Finite Element Model

One of the objectives of the current study was to compare the kinematic response of the pediatric cadaver cervical spine with that of the Hybrid III three-year-old child finite element model. In the event of significantly differing responses, the material properties of the pediatric cervical spine were incorporated into the neck of the Hybrid III model in an attempt to improve the biofidelity of the neck response. To accomplish this, material type 67 (*MAT_NONLINEAR_ELASTIC_DISCRETE_BEAM) was used. This material model is appropriate for simulating the linear and non-linear elastic and viscous characteristics of material and allows for translational and rotational stiffness to be modeled. Then material model allows the use of tensile force verses displacement curves to define the tensile force verses displacement response. As such, we used the tensile force verses displacement data previously obtained by averaging the pediatric cadaver cervical spine response to tensile loading.

Implementation of pediatric cadaver data would result in a more appropriate biofidelic neck of the Hybrid III model. These two Hybrid III three-year-old finite element models could be then subjected to frontal impact crash conditions consistent with those used by Kallieris et al, (1976). The resultant head and chest acceleration time profiles, upper and lower neck loads and moments and HIC was compared to determine

the degree of agreement between the two models and the models to experimental pediatric cadaver data from Kallieris et al. (1976).

5. RESULTS

5.1 Head and Neck Component Test Analysis

5.1.1 Linear Stiffness

Head and neck component testing was performed for the Hybrid III three-year-old altered and unaltered FE models under conditions similar to the axial distraction experimental procedure outlined by Ouyang et al. (2005) to validate the kinematic response of the altered model. Results of axial distraction loading are illustrated in Figures 6 and 7. Figure 6 contains the altered, unaltered and pediatric data whereas Figure 7 contains only the altered and pediatric data. A load versus deflection curve yields a maximum load at 13 mm displacement of 185 kN for the unaltered model, 450 N for the altered model and 425 N for the average pediatric cadaver data.

The altered model and pediatric data exhibited similar linear load-deflection profiles and the maximum values were within 6 percent difference of one another. Least Squares Linear Regression Analysis was utilized to compare the slopes (stiffness) of the unaltered, altered and pediatric load-deflection curves. The resulting slopes (stiffness) were 14,413 N/mm for the unaltered model, 34.5 N/mm for the altered model and 32.5 N/mm for the pediatric data. The numerically calculated stiffness for the altered model and the sub set of pediatric data used in this research are both in good agreement with the average stiffness calculated by Ouyang et al. (2005) of 34.7 N/mm.

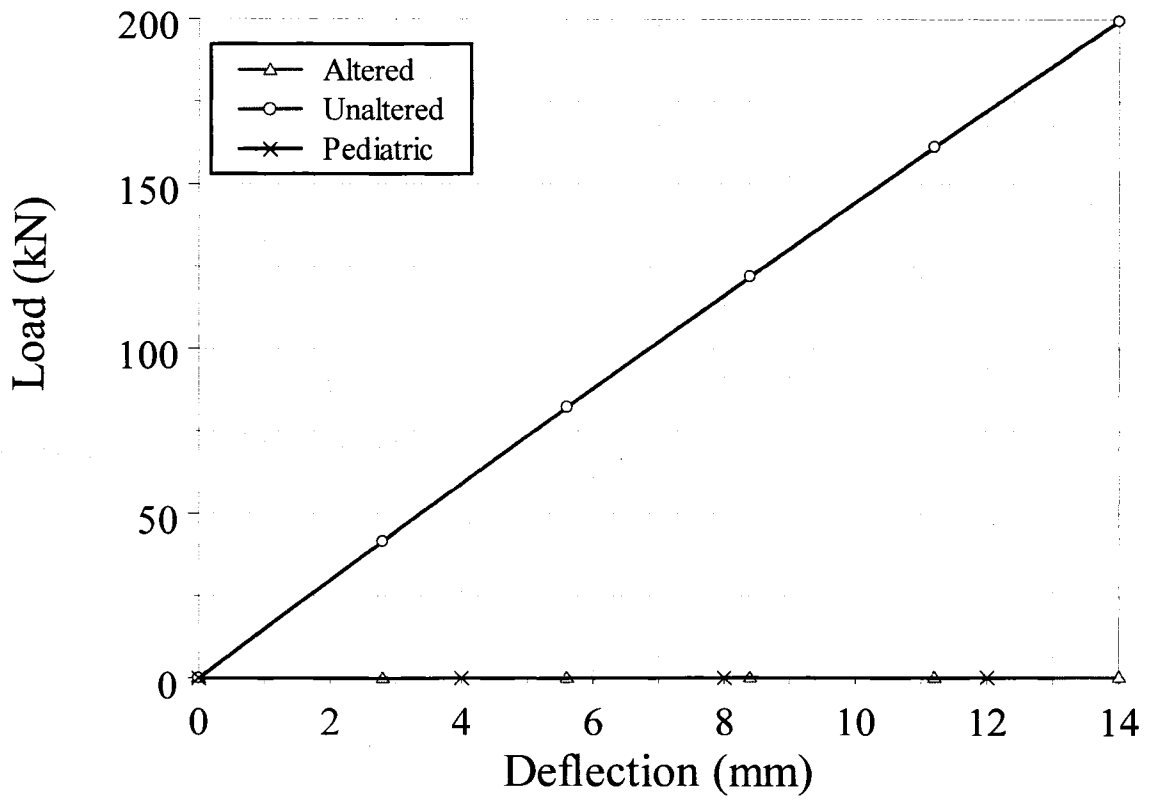


Figure 6. Axial neck force load-deflection curve for altered, unaltered and pediatric data.

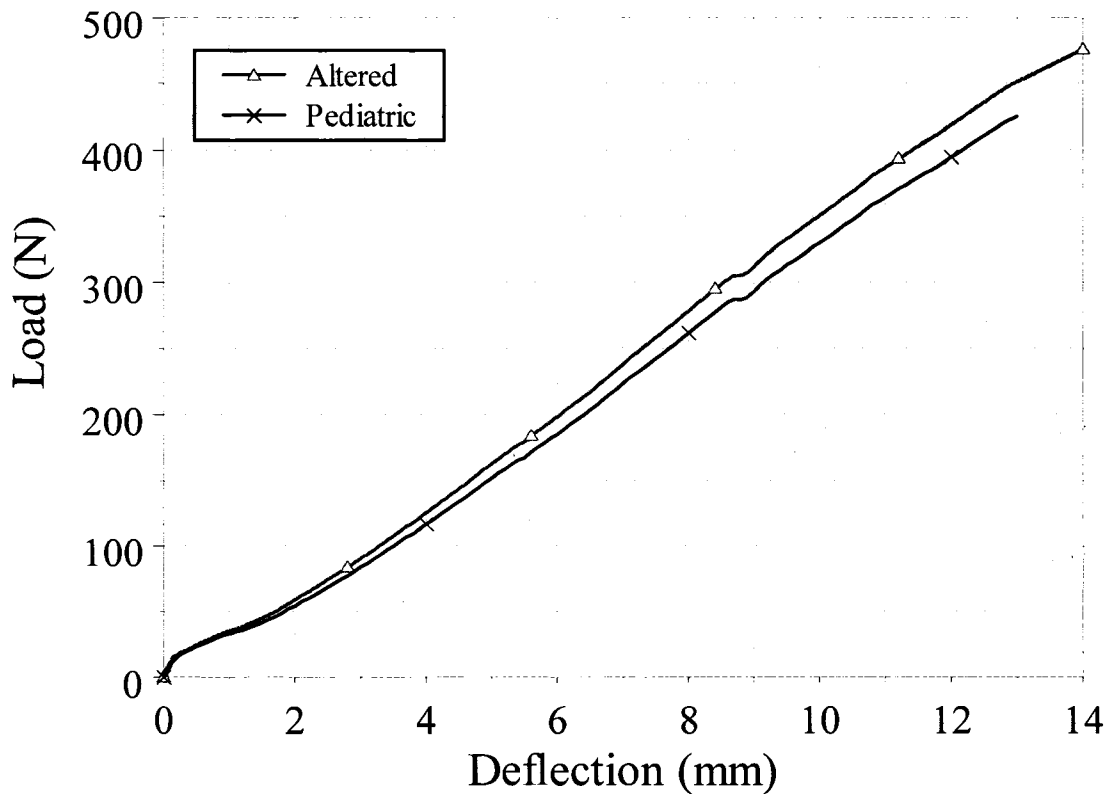


Figure 7. Axial neck force load-deflection curve for altered and pediatric data.

5.1.2 Angular Stiffness

Further head and neck component testing validation was performed for the Hybrid III three-year-old altered and unaltered FE models under conditions similar to the flexion-extension bending experimental procedure outlined by Oyuang et al. (2005). Analyses of the kinematic response under flexion-extension bending are illustrated in Figures 8 and 9. Figure 8 contains the altered, unaltered and pediatric data whereas Figure 9 contains only the altered and pediatric data. The unaltered model exhibited the greatest flexion-extension bending moments, 29.7 N·m for flexion and 11.4 N·m for extension. The unaltered model percentage difference was 168 percent and 128 percent greater for flexion and extension respectfully as compared to the pediatric data.

Conversely, the results of the altered model as compared to the unaltered model were in excellent agreement with those of the pediatric data. The altered model exhibited flexion-extension bending moments of 2.6 N·m for flexion and 2.4 N·m for extension. The percentage differences were 8 percent and 4 percent greater for flexion and extension respectfully as compared to the pediatric data. The experimentally obtained flexion extension bending moments for the pediatric data were 2.4 N·m for flexion and extension. In addition, the average rotational stiffness was calculated using Least Squares Regression Analysis for the altered model and was 0.04 N·m/deg which was identical to the calculated value of 0.04 N·m /deg for the experimental pediatric cadaver data as reported by Ouyang et al. (2005).

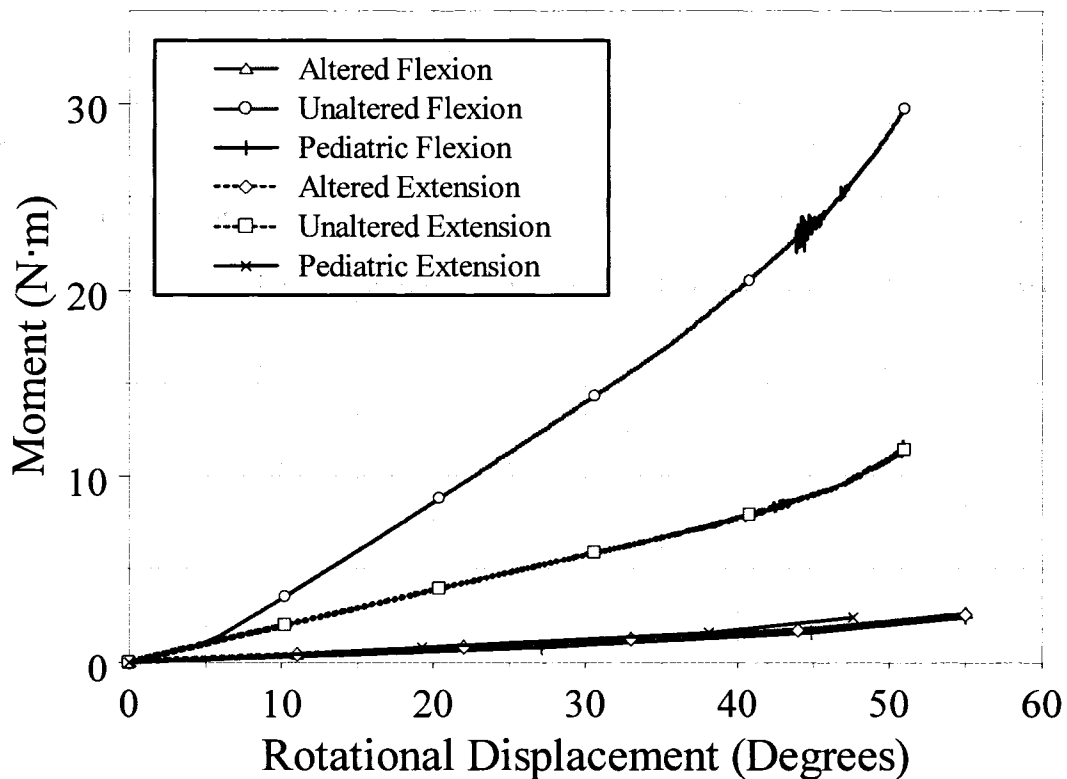


Figure 8. Angular neck moment load vs. rotational displacement curve for altered, unaltered and pediatric data under flexion and extension bending.

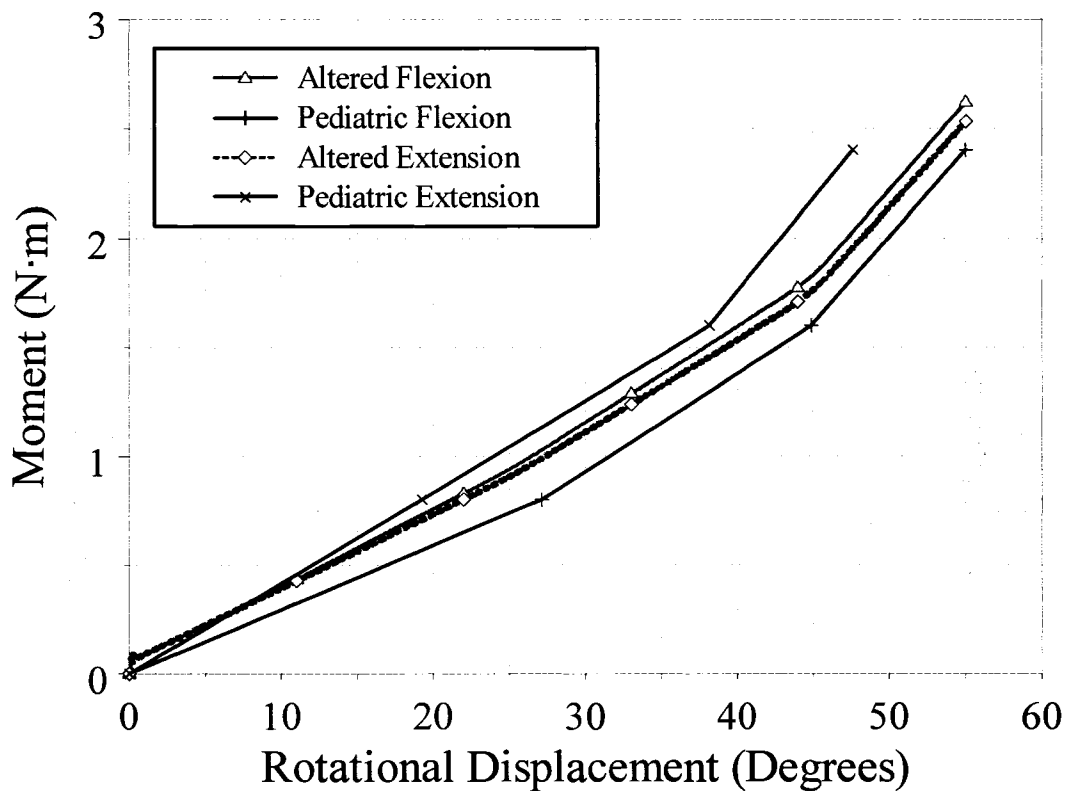


Figure 9. Angular neck moment load vs. rotational displacement curve for altered and pediatric data under flexion and extension bending.

5.2 Qualitative Kinematic Crash Analysis

A qualitative frame by frame analysis of the kinematic response of the altered and unaltered Hybrid III three-year-old FE models was completed. The results are illustrated in Figures 10 (side view) and 11 (cross sectional view). Both models exhibited a similar response, however, a greater degree of head rotation, neck flexion and chest deflection were observed for the altered model as compared to the unaltered model. Examination of the frames at 72 ms indicate the most notable difference was the degree of head rotation. This greater degree of head rotation observed in the altered models is more consistent with observations from other child dummy models such as the child finite element model and the Q3 finite element model.

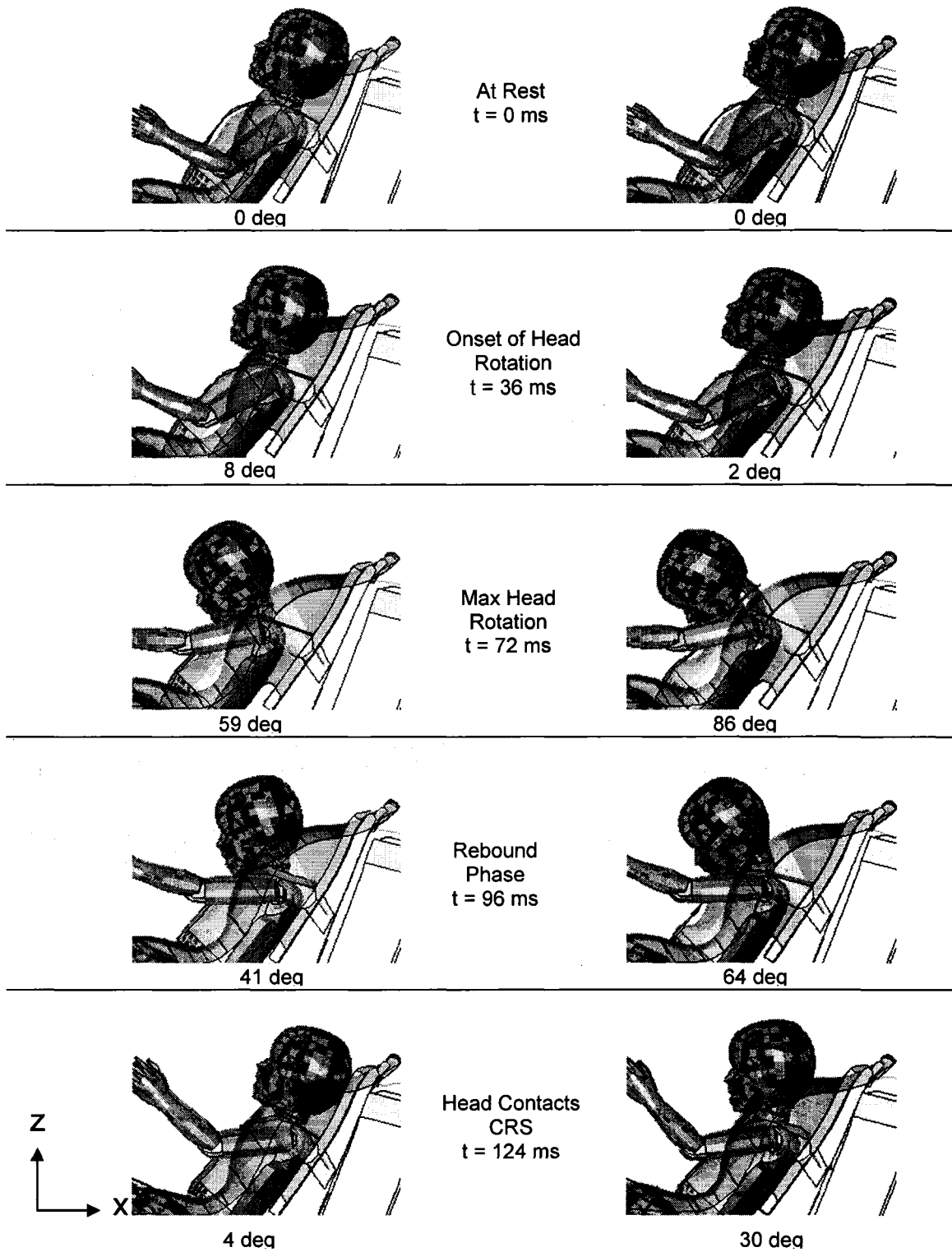


Figure 10. Frame by frame comparative analysis of unaltered (left) vs. altered (right) models.

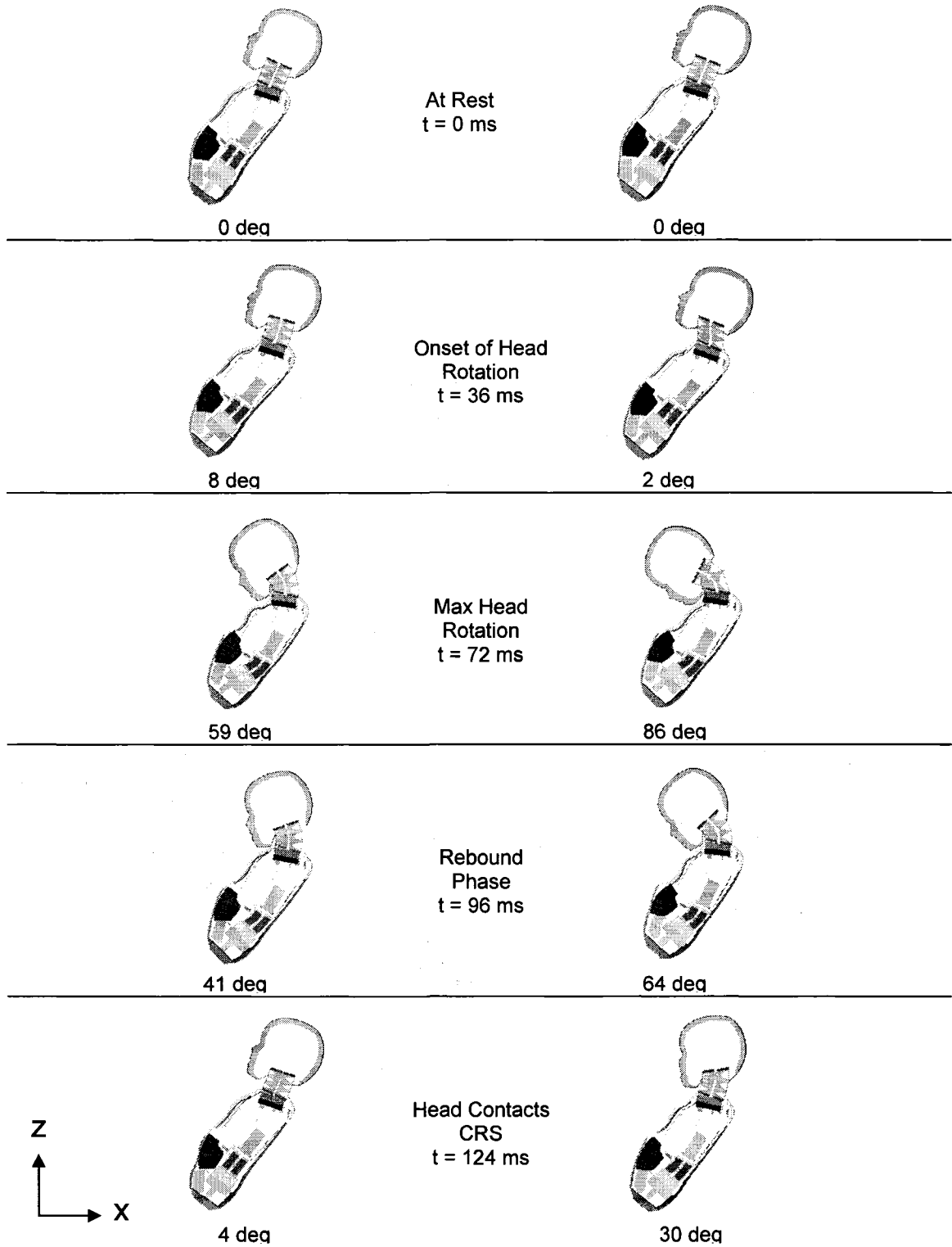


Figure 11. Cross sectional comparative analysis of unaltered (left) vs. altered (right) models.

5.3 Quantitative Kinematic Crash Analysis

5.3.1 Head Acceleration

The local x component of the head acceleration verses time for the altered and unaltered models are illustrated in Figure 12. Both models exhibited a similar acceleration profile with the most notable difference being a rapid change in acceleration for the altered model at 60 ms and a prominent maximum peak for the unaltered model at 130 ms. The minimum peak local x acceleration of the head was -47 g for the altered model and -40 g for the unaltered model. The time to peak for the local x acceleration minimum value was 67 ms for the altered model and 65 ms for the unaltered model. A phase shift of 2 ms for the altered model was observed for the time to reach minimum peak values. The duration of the peaks were approximately 14 ms which was followed by an upward ramp to a value of -21 g at 76 ms. The maximum peak occurred at 128 ms with a magnitude of 6 g for the altered model and at 137 ms with a magnitude of 37 g for the unaltered model.

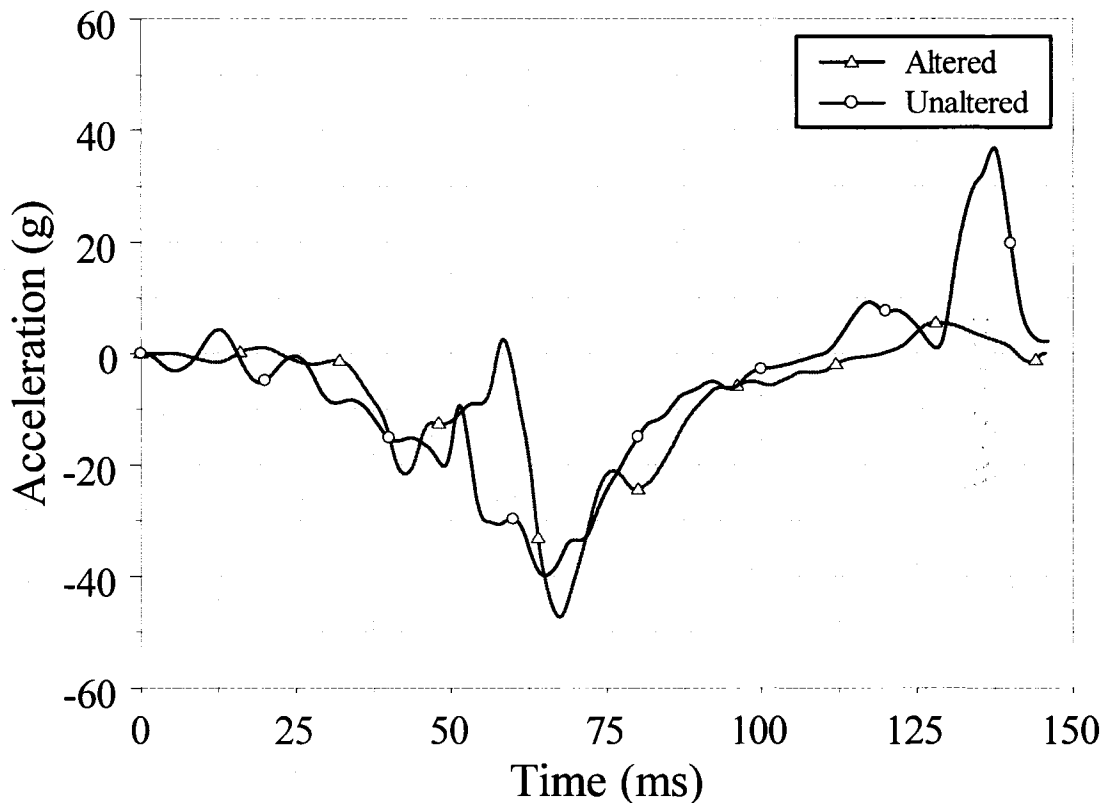


Figure 12. Head acceleration in the local x direction.

The local z component of the head acceleration versus time for the altered and unaltered models are illustrated in Figure 13. Both models exhibited a similar acceleration profile with the exception of a greater maximum peak value for the altered model. The maximum peak local z acceleration of the head was 82 g for the altered model and 25 g for the unaltered model. The time to peak for the local z acceleration minimum value was 58 ms for the altered model and 69 ms for the unaltered model. A phase shift for the unaltered model of 11 ms was observed for the time to reach maximum peak. The duration of the peak was approximately 5 ms for the altered model followed by a downward ramp starting at 69 ms to a value of 35 g. The duration of the peak for the unaltered model was 30 ms followed by a downward ramp starting at 70 ms. A second

peak occurred at 142 ms with a magnitude of 16 g for the altered and at 132 ms with a magnitude of 18 g for the unaltered model. The direction of the phase shift for the second peak was consistent with that of the first peak and the magnitude was 10 ms.

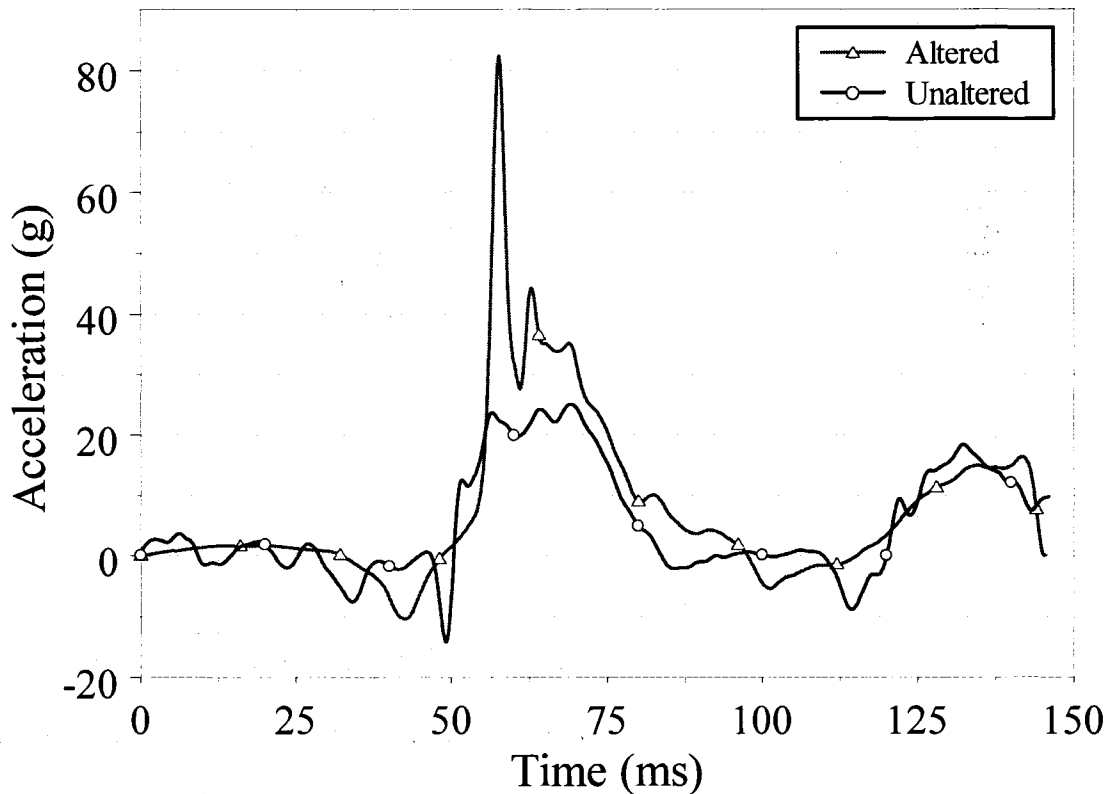


Figure 13. Head acceleration in the local z direction.

The resultant head acceleration verses time for the altered and unaltered models are illustrated in Figure 14. Both models exhibited a similar acceleration profile with the exception of a greater maximum peak value for the altered model and a greater second maximum peak for the unaltered model. The maximum resultant peak acceleration of the head was 82 g for the altered model and 47 g for the unaltered model. The time to peak for the local x acceleration minimum value was 58 ms for the altered model and 65 ms for the unaltered model. A phase shift of 7 ms was observed for the unaltered model. The

duration of the peak was approximately 5 ms for the altered model followed by a downward ramp starting at 69 ms to a value of 35 g. The duration of the peak for the unaltered model was 30 ms followed by a downward ramp starting at 70 ms.

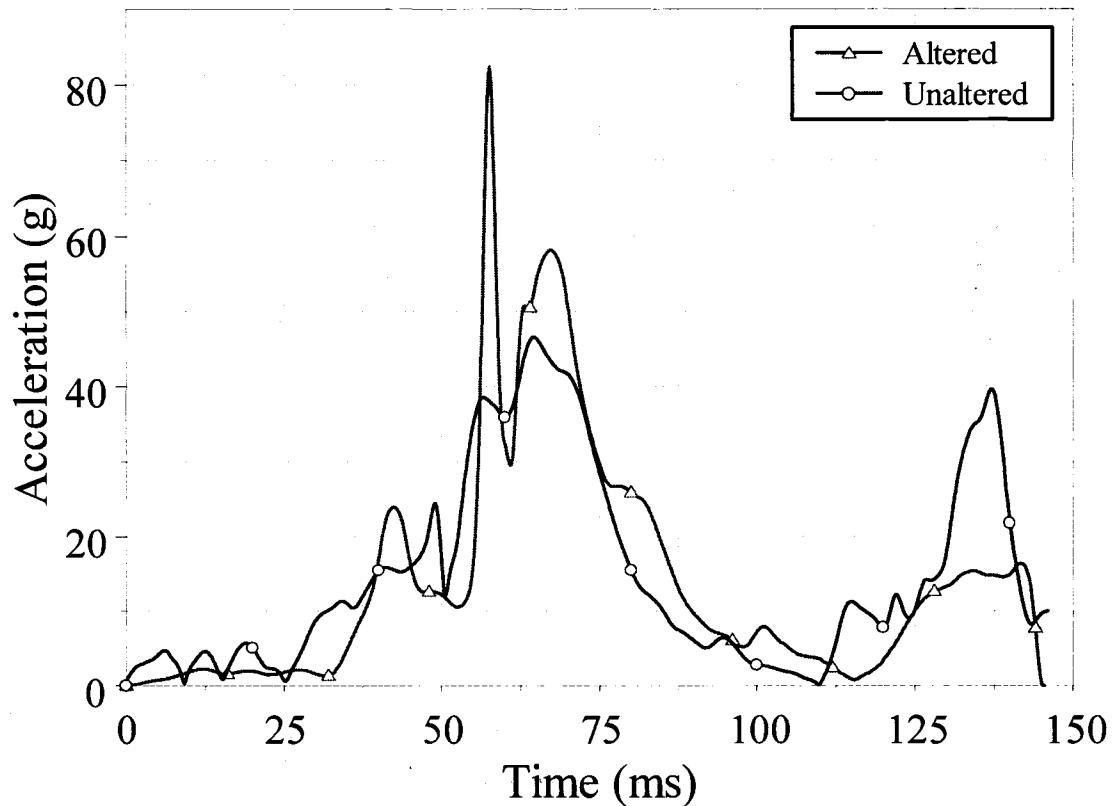


Figure 14. Resultant head acceleration.

5.3.2 Chest Acceleration

The local x component of the chest acceleration verses time for the altered and unaltered models are illustrated in Figure 15. The curves exhibited similar acceleration profiles with the most notable difference again being a rapid acceleration change for the altered model occurring at 58 ms and a more prominent maximum peak for the unaltered model occurring at 113 ms. The minimum local x acceleration for the altered model was -40 g and -29 g for the unaltered model. The time to minimum peak was 52 ms and the

duration of the peak was 5 ms for both models. The local x acceleration maximum peak chest acceleration for the altered model occurred at 9 ms and was 16 g in magnitude while the maximum local x chest acceleration for the unaltered model occurred at 112 ms and was 18 g in magnitude.

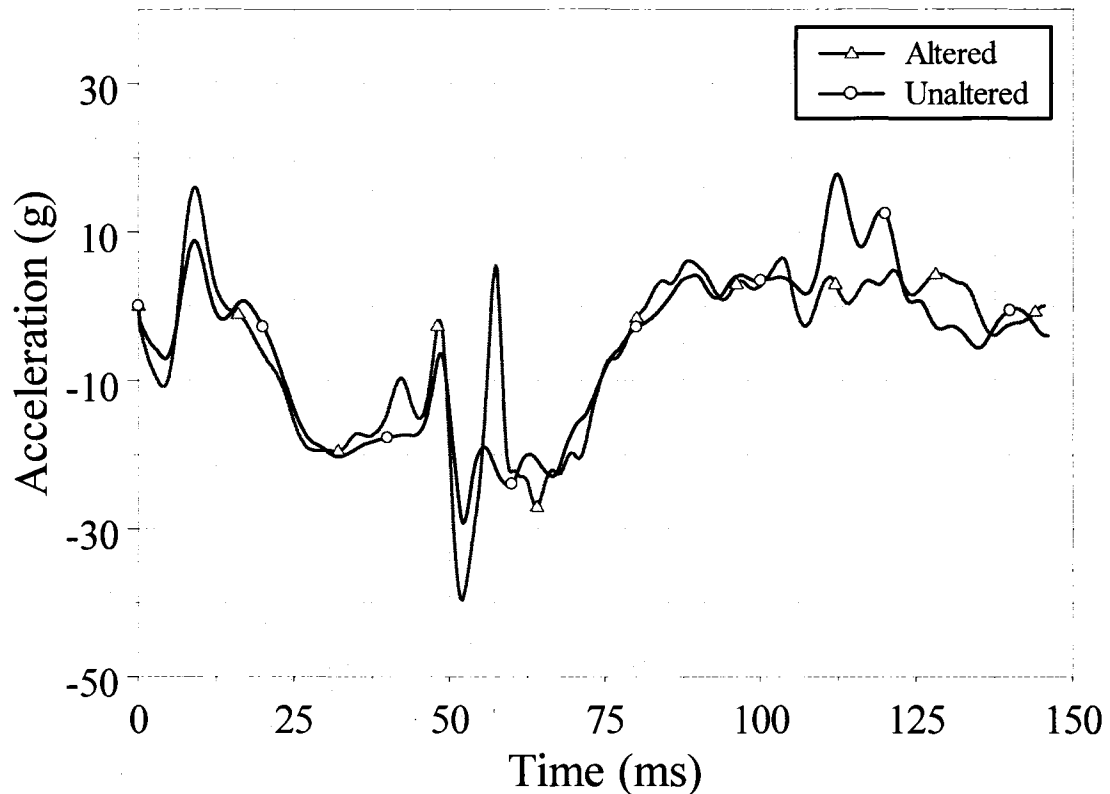


Figure 15. Chest acceleration in the local x direction.

The local z component of the chest acceleration verses time for the altered and unaltered models are illustrated in Figure 16. The curves followed similar acceleration profiles. The altered model exhibited greater minimum and maximum values and oscillated about the unaltered model. The minimum local z acceleration for the altered model was -38 g and -26 g for the unaltered model. The time to minimum peak was 58 ms for the altered model and 48 ms for the unaltered model. The duration of the peak was

4 ms for both models. The local z acceleration maximum peak chest acceleration for the altered model occurred at 67 ms and was 17 g in magnitude while the maximum local z chest acceleration for the unaltered model occurred at 141 ms and was 10 g in magnitude.

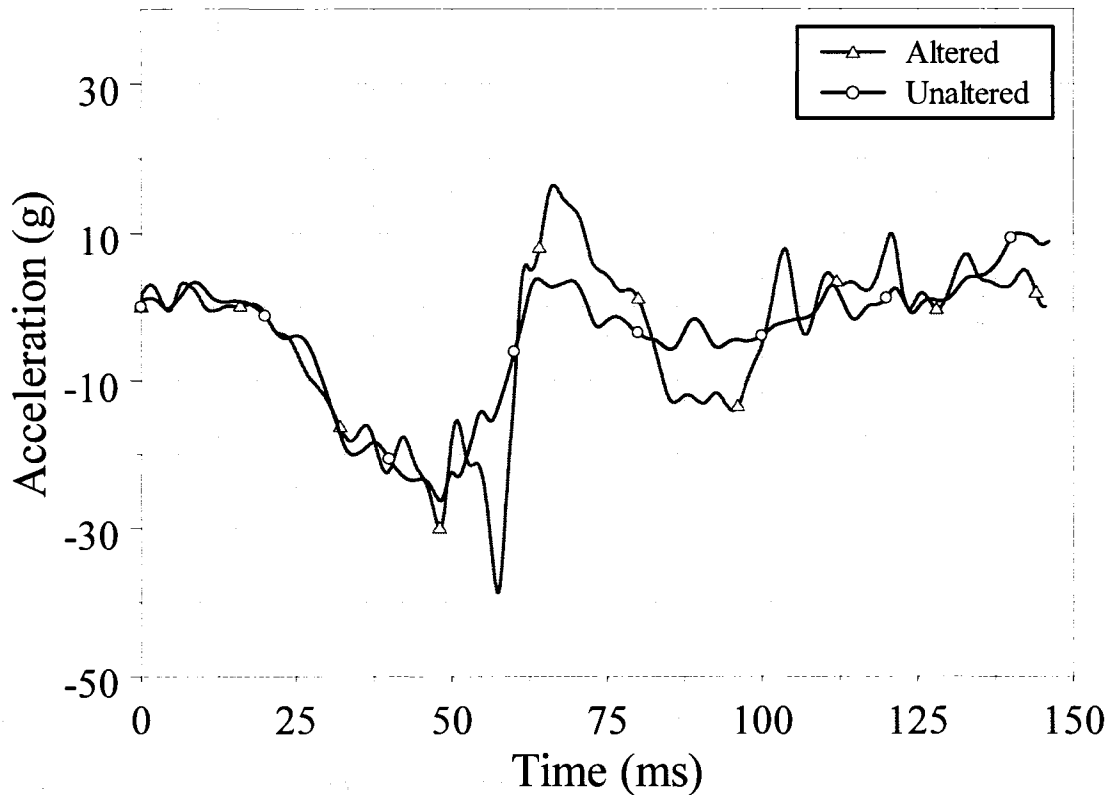


Figure 16. Chest acceleration in the local z direction.

The resultant head acceleration verses time for the altered and unaltered models are illustrated in Figure 17. The models exhibited similar acceleration profiles with the exception of the second set of sub maximum resultant peaks occurring at differing times. The maximum resultant peak acceleration of the chest was 44 g for the altered model and 36 g for the unaltered model. The time to peak for the resultant acceleration was 52 ms for both the altered and unaltered models. The duration of the peaks was 6 ms for both models. A second sub maximum peak for the altered model occurred at 95 ms and had a

magnitude of 14 g. The second sub maximum peak for the unaltered model occurred at 112 ms and was 18 g in magnitude.

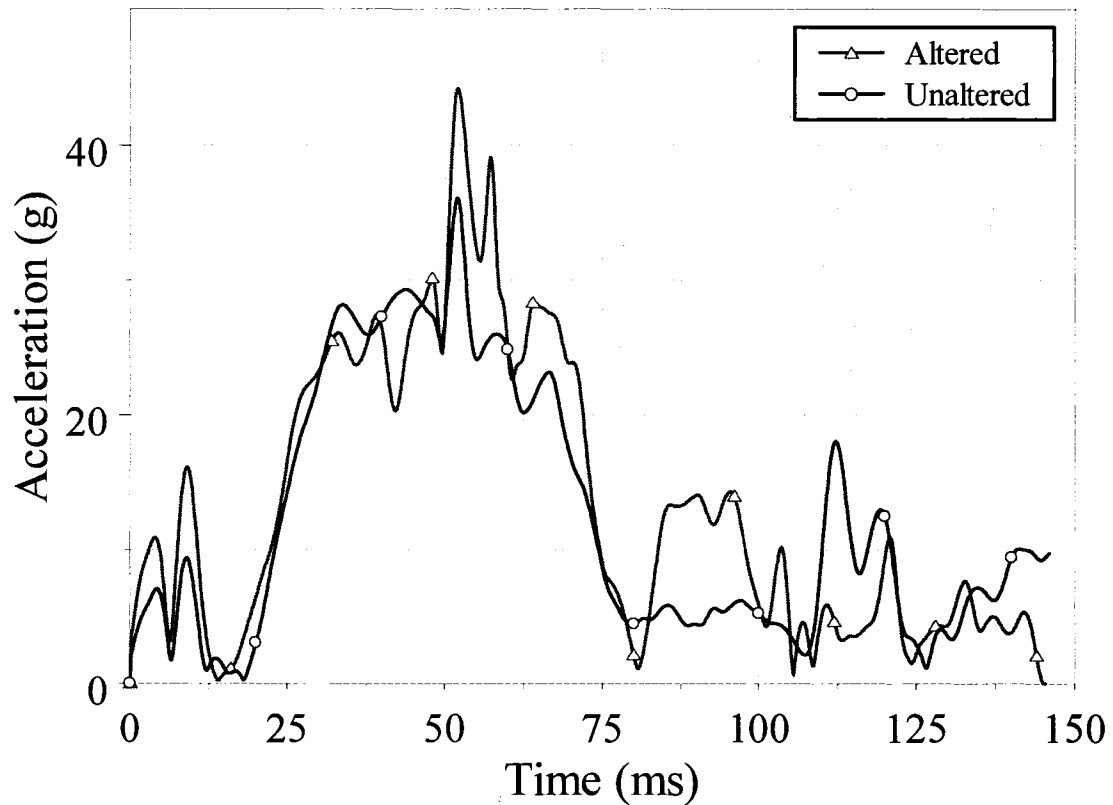


Figure 17. Resultant chest acceleration.

5.3.3 Chest Deflection

A greater degree of chest deflection was observed for the altered model as compared to the unaltered model. The maximum chest deflection for the altered model was observed to be 15 mm at 74 ms whereas the unaltered model exhibited a maximum chest deflection of 6 mm at 42 ms. The time to peak for the altered model was 74 ms as compared to 42 ms for the unaltered model. The altered model CTI was 141 percent greater than the unaltered model. The values for the CTI were 0.81 and 0.57 for the altered and unaltered models respectfully.

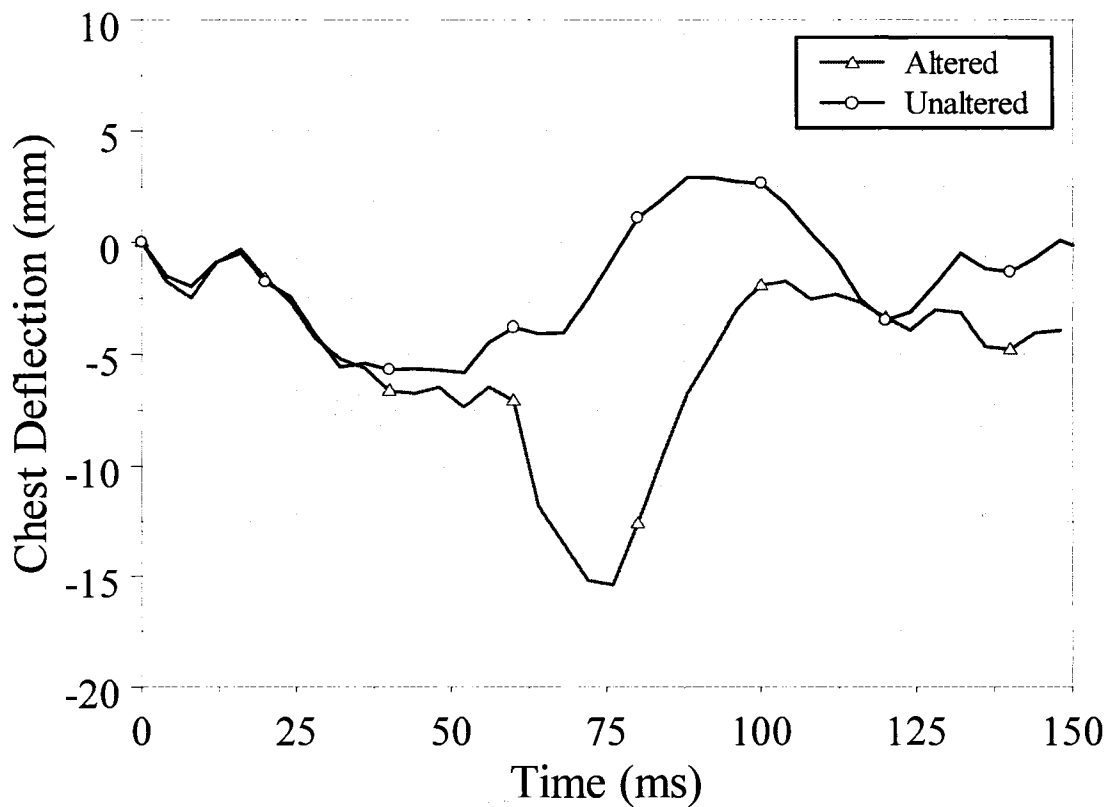


Figure 18. Chest deflection.

5.3.4 Neck Forces

The resultant upper and lower neck forces as a function of time for the altered and unaltered models are illustrated in Figures 19 and 20. The values for the upper neck peak maximum forces were 2321 N for the altered model and 1732 N for the unaltered model. The values for the lower neck peak forces were 1692 N for the altered model and 709 N for the unaltered model. The time to peak for the upper neck forces was 69 ms for the altered model and 65 ms for the unaltered model. The time to peak for the lower neck forces were 58 ms for the altered model and 49 ms for the unaltered model. The duration of the peaks for the upper neck force was 43 ms for the altered model and 33 ms for the

unaltered model. The duration of the peak for the lower neck forces was 100 ms for the altered model and 40 ms for the unaltered model. In addition, the altered model peak maximum neck forces were greater than the unaltered model neck forces. The duration of the peak neck force was approximately 50 ms for both the upper and lower altered and unaltered models.

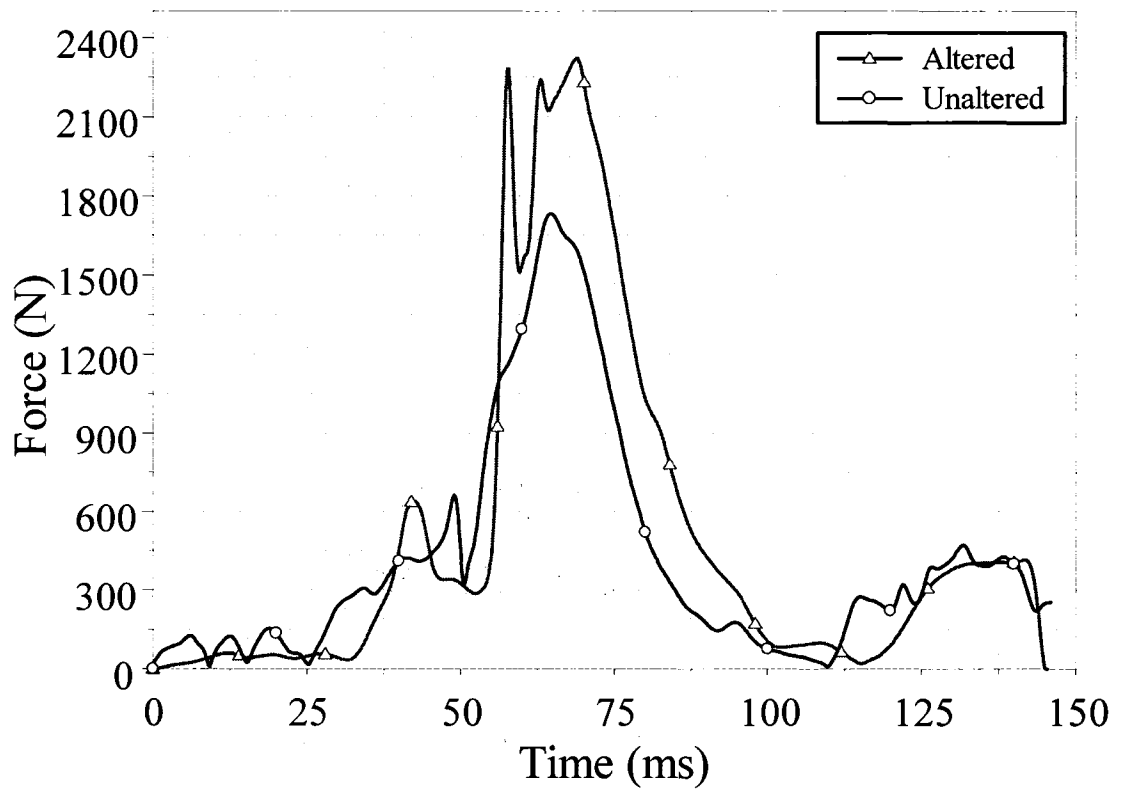


Figure 19. Resultant upper neck force.

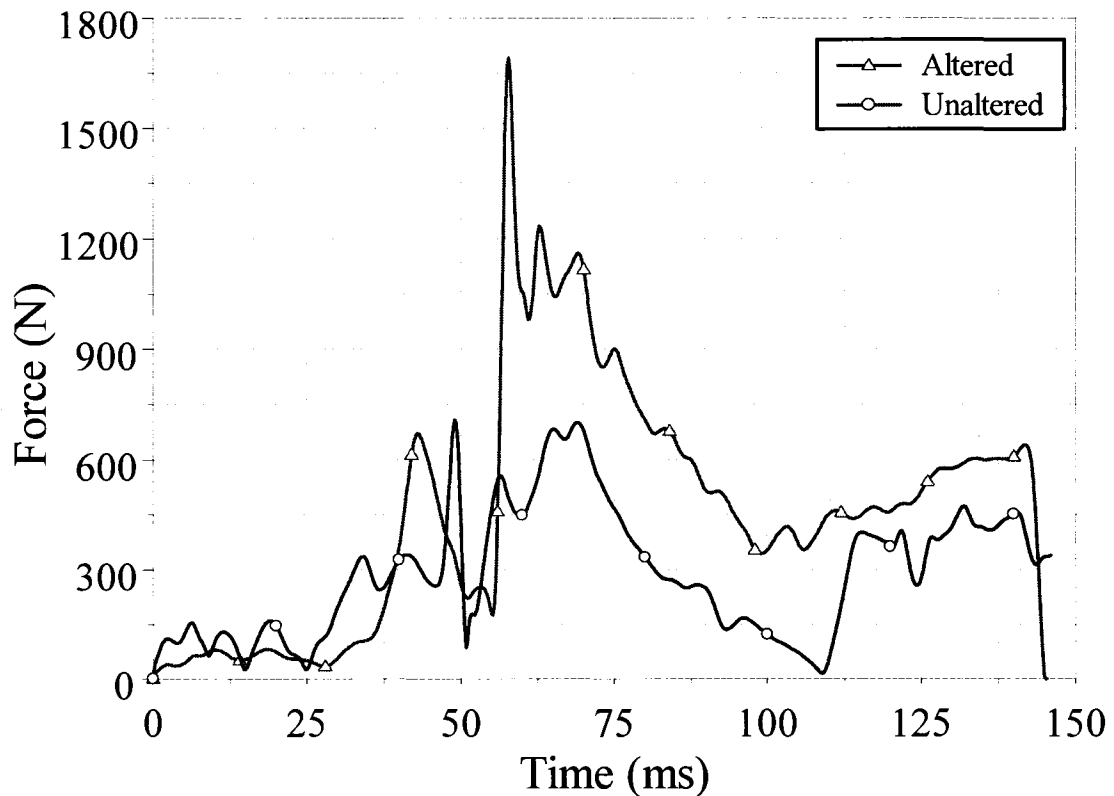


Figure 20. Resultant lower neck force.

5.3.5 Neck Moments

The resultant upper and lower neck moments as a function of time for the altered and unaltered models are illustrated in Figures 21 and 22. The values for the upper neck peak maximum moments were similar, although the upper neck resultant moment profiles presented notable differences. The upper neck resultant moments exhibited a time shift of approximately 8 ms for the unaltered model and the emergence of relatively large secondary and tertiary sub maximal peaks at 116 ms and 138 ms respectively. The upper neck moment for the altered and unaltered models was 31 N·m. The time to peak for the altered model upper neck moment was 43 ms and the time to peak for the upper neck moment for the unaltered model was 51 ms. The lower neck moments for the altered and

unaltered models were significantly greater than the upper neck moments and were 122 N·m and 134 N·m respectively. The duration of the peak neck force was approximately 50 ms for both the upper and lower altered and unaltered models.

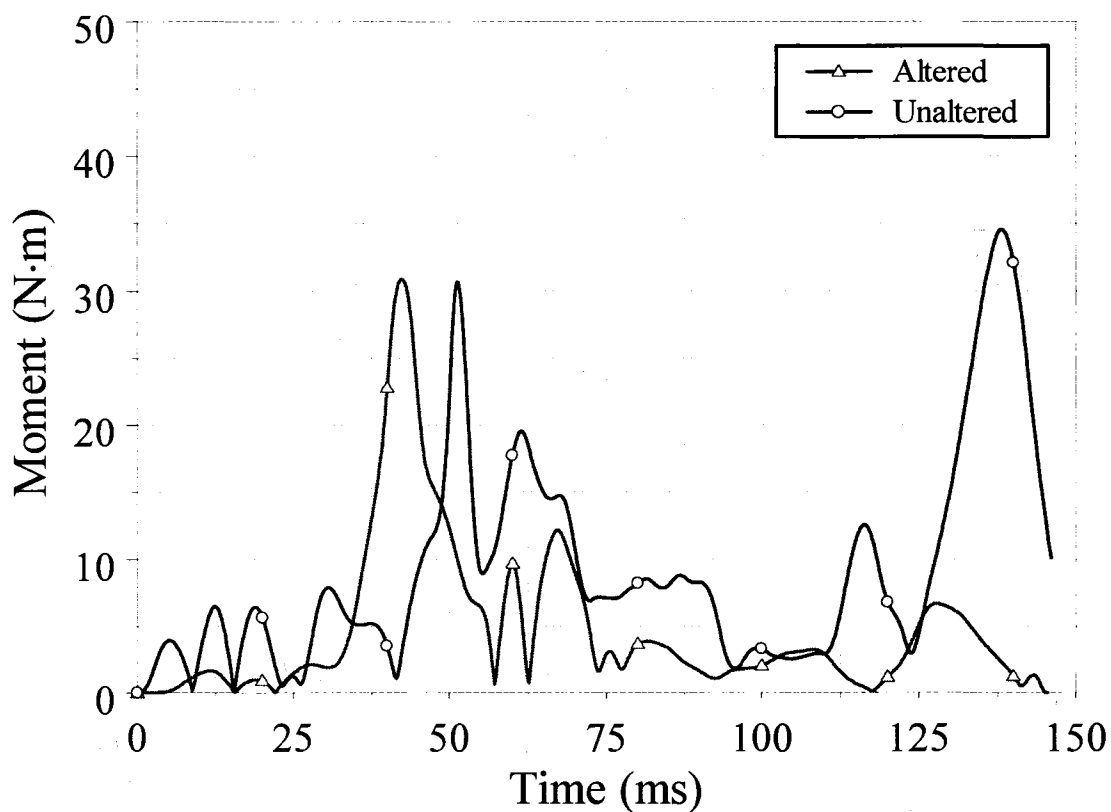


Figure 21. Resultant upper neck moment.

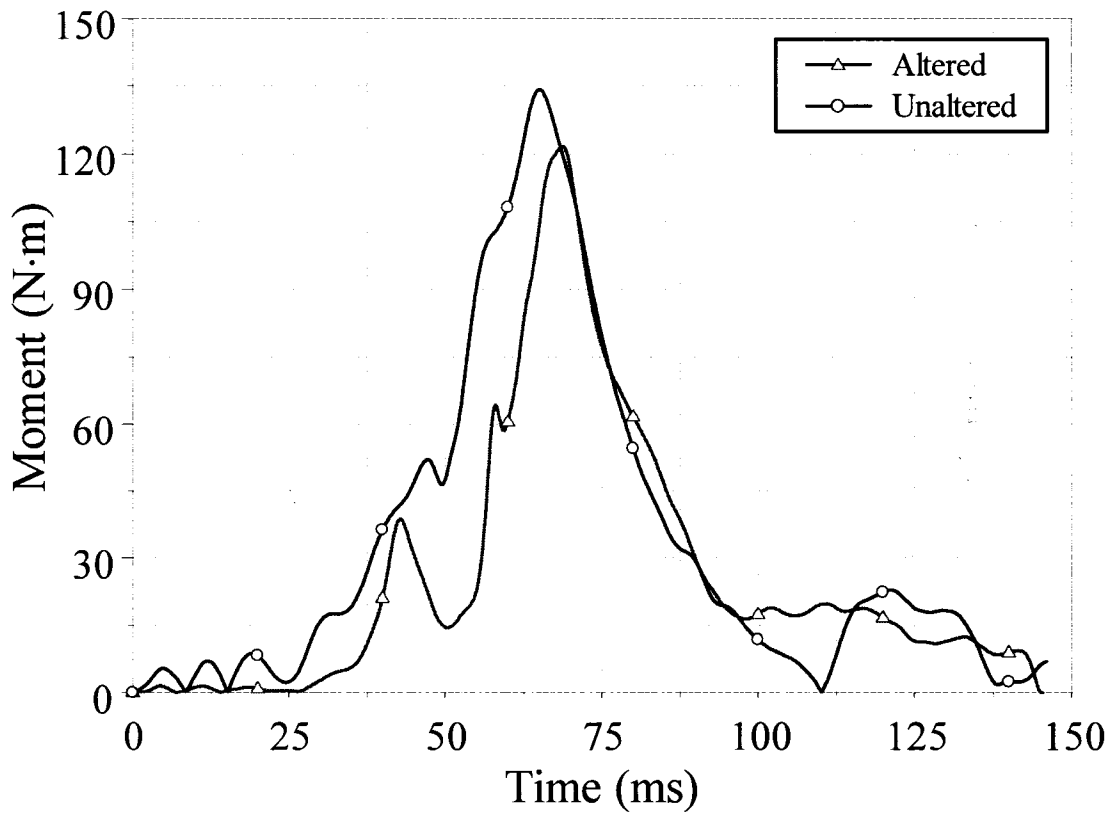


Figure 22. Resultant lower neck moment.

5.3.6 Head Injury Criteria

The head injury criteria were calculated over a 15 ms and 36 ms window for the altered and unaltered models. The values for the HIC are illustrated in Figure 23. The HIC was greater for the altered model than the unaltered model. The HIC_{15} for the altered model was 286 as compared to 162 for the unaltered model. The HIC_{36} was 268 for the altered as compared to 194 for the unaltered model.

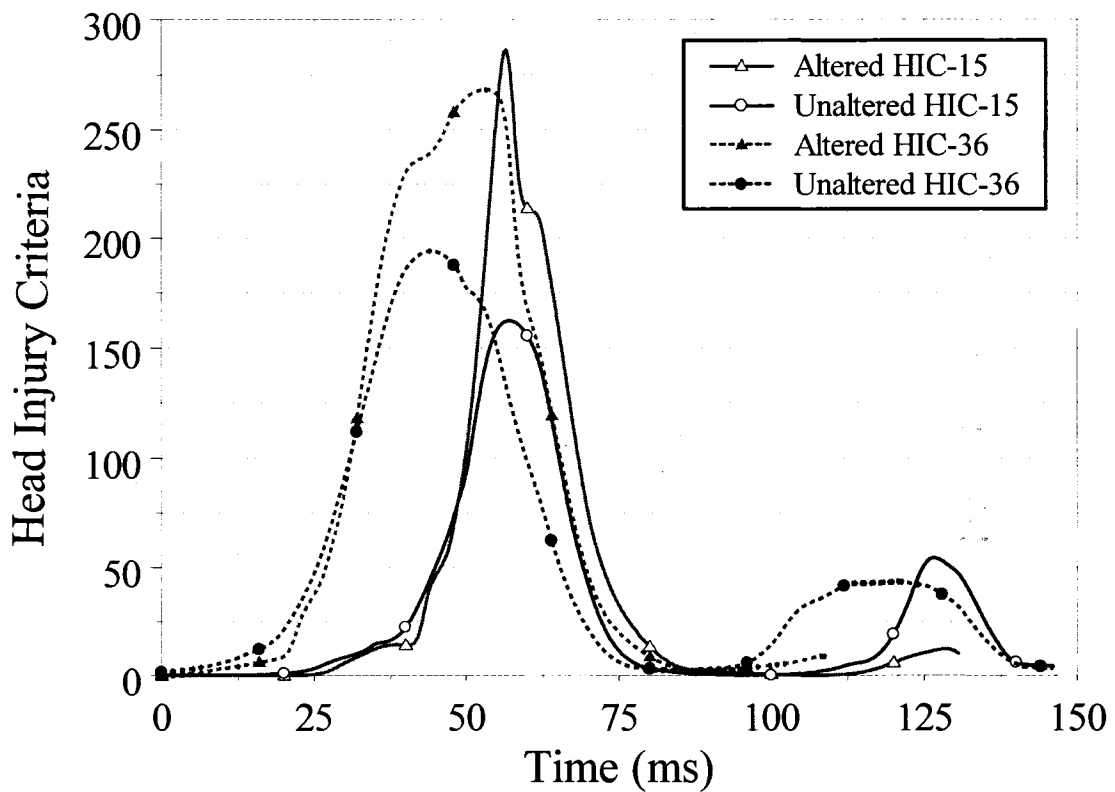


Figure 23. Head injury criteria.

5.3.7 Head Rotation

The maximum rotation of the centre of gravity of the head was observed to be greater for the altered model as compared to the unaltered model. The altered model exhibited a maximum head rotation of 86 degrees at 75 ms. The unaltered model exhibited 60 degrees of rotation at 70 ms.

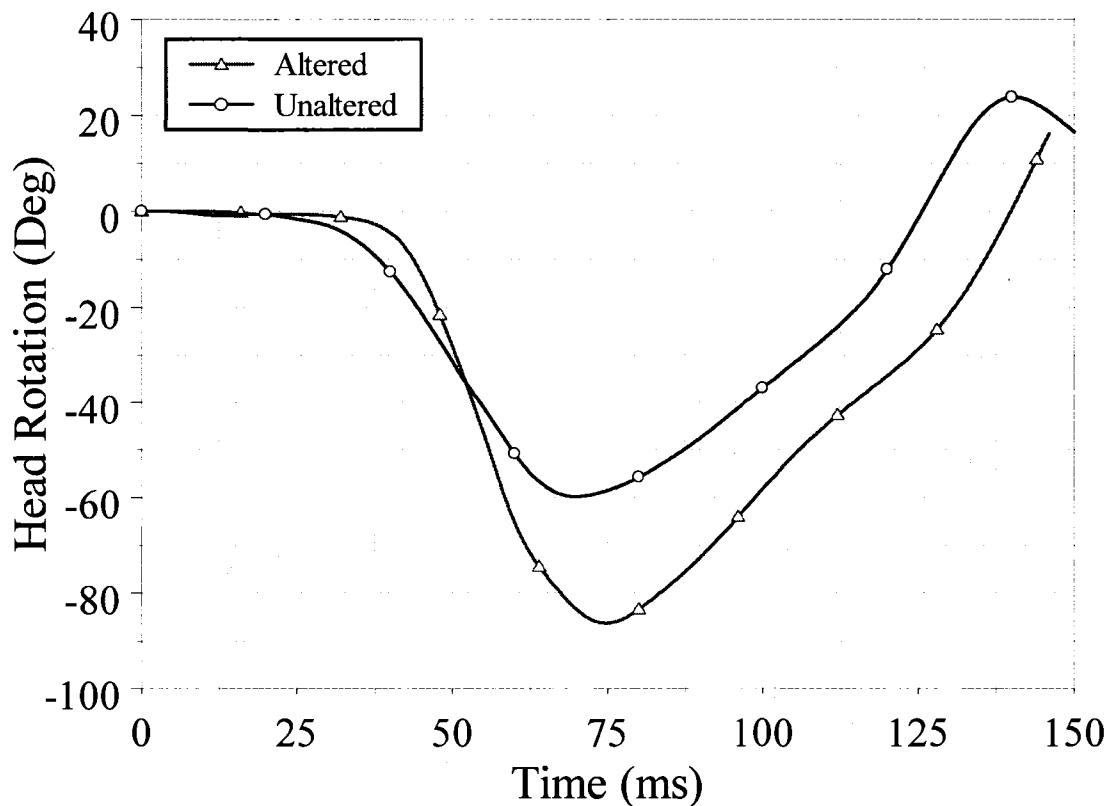


Figure 24. Head rotation.

5.3.8 Head Trajectory

Analysis of head trajectory is illustrated in Figure 25 which shows a greater degree of displacement for the altered model as compared to the unaltered model which more closely resembles the profile of the trajectory of the pediatric cadaver data from Kallieris et al. (1976). The local (x,z) displacement ordered pairs for the altered model at maximum trajectory are (230 mm, 138 mm) and (196 mm, 85 mm) for the unaltered model. The maximum trajectory for the pediatric cadaver data was (364 mm, 227 mm). The maximum local x excursion of the head for the models and cadaver data were less than the recommended maximum value of 720 mm as cited in Federal Motor Vehicle Safety Standard 213.

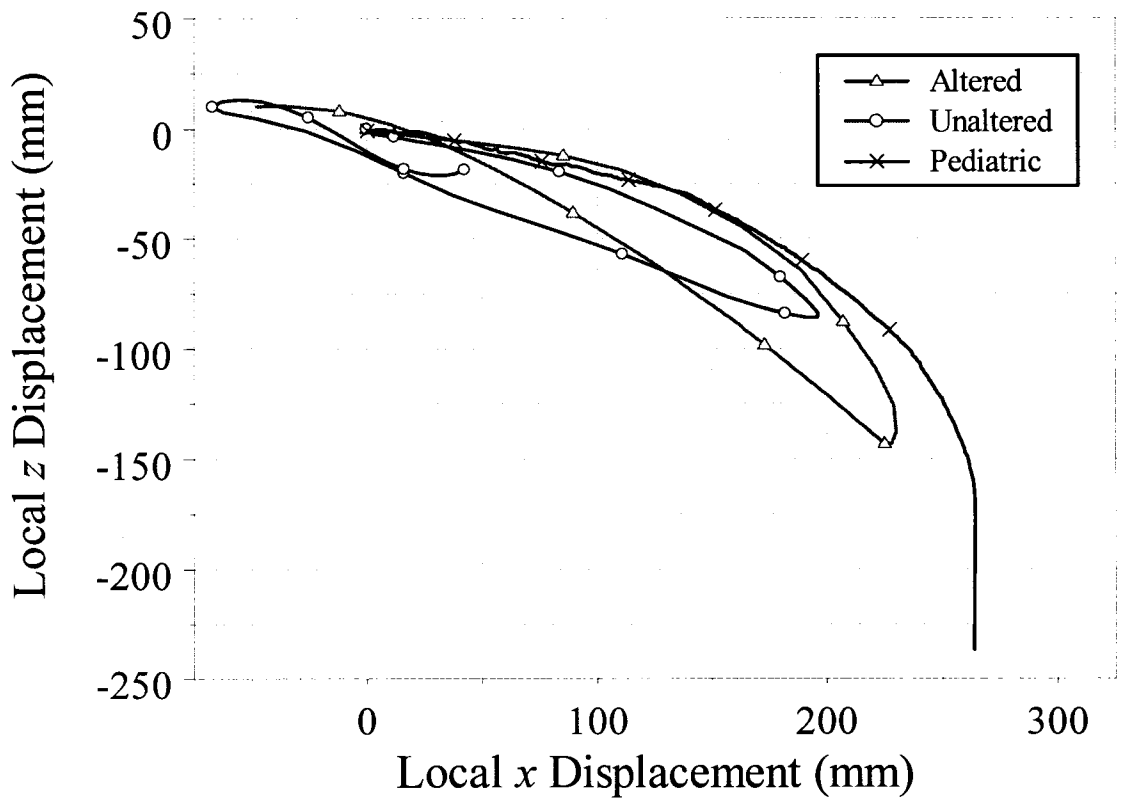


Figure 25. Head trajectory.

6. DISCUSSION

6.1 Head and Neck Component Test Analysis

6.1.1 Linear Stiffness

The purpose of the component testing was to determine if a significant difference in axial stiffness exists between the neck of the Hybrid III three-year-old model and the pediatric cadaver data. In solid mechanics, Young's modulus (E) is a measure of the stiffness of a material. It is defined as the ratio, for elastic strains, of stress to strain. Briefly, stress is a measure of force per unit area acting on or within a material. Strain is a uniaxial entity, and is the change in length of a material normalized with respect to its original length. The stiffness of a material can be experimentally determined from the slope of a load-deflection curve during a tensile or compressive test conducted on a sample of the material. For the altered and unaltered models a load-deflection curve revealed a significant difference in stiffness which supported the directional first hypothesis and subsequent calibration of the model to the pediatric cadaver experimental test results ensued.

To calibrate the model, the average load-deflection curve for the pediatric cadaver data was implemented into the material properties of the neck of the Hybrid III FE model. All materials were assumed to be isotropic. Further testing validated the response of the model was within 6 percent of the pediatric cadaver data when comparing the load at 13 mm deflection. The results are illustrated in Figures 6 and 7.

6.1.2 Angular Stiffness

With the linear load-deflection material properties implemented and validated in the Hybrid III FE model, initial testing was conducted to determine if a difference existed

between the Hybrid III altered and unaltered models and the pediatric cadaver data for flexion-extension bending. When materials are subjected to bending, a shear stress and strain are developed. Shear stresses and strains are developed when the stress or strain acts parallel to the face of the material. In materials science, shear modulus, G , is defined as the ratio of shear stress to shear strain.

Despite the Hybrid III having the linear load-deflection material properties implemented, the model exhibited a significantly greater bending moment for flexion-extension bending testing than that of the pediatric cadaver data. An iterative process was employed to reduce the material properties of the model, namely, the short time shear modulus, long time or infinite shear modulus and decay constant of the neck material to scale down the bending moment of the model. After several trials were completed, values for the material properties of the neck were identified that produced a flexion-extension bending moment that was in good agreement with that of the pediatric cadaver data. Load-deflection curves illustrated in Figures 7 and 8 show that at 55 degrees deflection the percentage difference was found to be 8 percent for the flexion moment and 4 percent for the extension moment. Differences between flexion and extension can be primarily attributed to the model geometry of the neck components and experimental error. With the linear and new angular material properties implemented in the model, linear distraction testing was again completed to ensure the new angular material properties did not significantly change the response of the model under axial distraction loading.

6.2 Qualitative Kinematic Crash Analysis

The Hybrid III three-year-old altered and unaltered models were positioned in a child restraint system FE model. Using LS-DYNA, the model was loaded with an acceleration pulse used by Kallieris et al. (1976) in an experimental child cadaver sled test. Frame by frame qualitative analyses were conducted for the altered and unaltered models. Although both models exhibited similar kinematic responses, from the side view it was evident that the altered model exhibited a 31 percent greater degree of head rotation. The greater degree of head rotation is primarily due to the neck parts having reduced material stiffness properties for the altered model.

By examination of the cross sectional views of the altered and unaltered models, it is evident that a shearing phenomenon is occurring in the neck of the altered model at the onset of head rotation at approximately 36 ms. This biomechanical response exhibited by the altered model is more consistent with the injury mechanism of AOD. In addition, it was determined from the cross sectional views that the altered model exhibited a 141 percent greater degree of chest deflection which can be attributed to the head having a greater degree of rotational displacement and subsequent contact with the chest.

6.3 Quantitative Kinematic Crash Analysis

6.3.1 Head Acceleration

The magnitude of the minimum local x , maximum local z and resultant peaks were greater for the altered model as compared to the unaltered model. This may be attributed to a greater rotational displacement of the head the altered model travels in the same amount of time as the unaltered model. In addition, rapid change in acceleration for the altered model on the local x , local z and resultant acceleration profiles may be

attributed to a whiplash phenomena experienced by the head during the crash. The minimum peak local x and maximum z components and resultant head acceleration for the altered and unaltered models occur at approximately the same time. For the altered model to achieve a greater displacement in the same amount of time requires a greater acceleration of the head. The minimum peak local x and maximum z components and resultant head acceleration peak events also coincide with the instant of maximum head rotation. In addition, the unaltered model exhibited a prominent local x acceleration maximum peak of 36 g at approximately 137 ms which was due to the head of the unaltered model making contact with the CRS whereas the altered model does not make contact with the CRS.

6.3.2 Chest Acceleration

The magnitude of the minimum peak local x and z components and the maximum resultant chest acceleration were greater for the altered model as compared to the unaltered model. These peaks occurred at approximately the same time which coincided with the approximate time of maximum head rotation. A prominent maximum peak was evident 112 ms for the unaltered model and represents the time of head contact with the CRS.

6.3.3 Chest Deflection

Chest Thoracic Index was 141 percent greater for the altered model as compared to the unaltered model. This can be attributed to a greater rotational displacement of the head of the altered model which contacts the chest causing a greater degree of deformation. The time of maximum chest deflection for the altered model of 72 ms more closely coincides with the maximum rotational displacement of the head of 74 ms as

opposed to the maximum local x acceleration of the chest which was 52 ms. The unaltered model deformation peaked at 42 ms which more closely coincides with the minimum local x chest acceleration of 52 ms.

The difference in the calculated values for CTI for the altered and unaltered models can be explained by a greater 3 ms peak resultant acceleration of the spinal cord for the altered model as compared to the unaltered model. In addition, the altered model exhibited greater chest deflection values as compared to the unaltered models. Since both terms are in the numerator of the CTI equation, increasing both values in the equation would increase the end resultant CTI value. It also stands to reason that with reduced linear and angular material stiffness properties in the neck of the altered model, there would be less resistance to rotation provided by the neck material to counteract the forward rotation of the head. With a greater degree of rotation, the head contacts the chest which compresses and counteracts some of the rotational forces of the head thereby increasing the chest deflection.

6.3.4 Neck Forces

Two trends emerged for the upper and lower neck forces; the altered model exhibited higher neck forces than the unaltered model and the upper neck forces were greater than the lower neck forces. The greater neck forces observed in the altered model are attributed to a greater acceleration of the head of the altered model as compared to the unaltered model. Since force is equal to the product of mass and acceleration, and since the mass of the head of the altered and unaltered models are equal, the greater acceleration of the head of the altered model produces greater upper and lower neck forces.

The upper neck forces being greater than the lower neck forces are primarily due to the force attenuation characteristics of the neck. The neck attenuates some of the forces between the upper neck load cell and the lower neck load cell. This results in less force being transmitted from the head to the lower neck. This observation was consistent with previous research conducted by Sances et al. (2002). An important point to note is that the forces and moments observed in the dynamic crash simulations are significantly greater than the forces and moments observed in the quasi static component test analysis and pediatric cadaver data. This can be attributed to the dynamic mass inertia effect of the head that is negligible in the quasi static numerical simulations and experiment. In addition, the loads predicted from the numerical simulation were significantly greater than the loads at failure for the pediatric cadaver data. This indicates that for the numerical crash test, catastrophic failure would have occurred in the neck region. Failure is not observed in the numerical simulation because LS-DYNA linearly extrapolates and exceeding the failure loads from the pediatric cadaver data.

6.3.5 Neck Moments

Two trends again emerged with respect to the upper and lower neck moments; the lower neck moment had a greater maximum peak value and a greater time to peak. The greater maximum peak value can be primarily attributed to two factors; the sum of the moments of the head and neck and the length of the moment arm acting on the lower neck. Firstly, the moment acting on the upper neck is due to the rotational moment of the head whereas the moment acting on the lower neck is due to the rotational moment of the head plus the rotational moment of each vertebral body in the neck. In addition, the distance the centre of mass of the head is from the axis of rotation, or in other words, the

length of the moment arm is greater for the lower neck load as opposed to the upper neck. This greater moment arm gives the mass of the head a greater mechanical advantage to generate a larger moment about the lower neck.

The greater time to peak for the lower neck moment as compared to the upper neck moment can be explained as follows. The upper neck reaches full rotation earlier than the lower neck. This is due to the successive rotation of each vertebral body in the neck and the time required until this mechanism is propagated to the lower neck. As the head begins to rotate, the upper neck achieves full segmental vertebral rotation prior to the lower neck which gives rise to an earlier peak moment for the upper neck as compared to the lower neck.

6.3.6 Head Injury Criteria

The altered model had greater values of the HIC_{15} and HIC_{36} as compared to the unaltered model. Since the HIC is an acceleration based criterion, it would be expected that the altered model which experienced a greater head acceleration and rotational displacement would produce a greater value for the HIC. For the altered model, the HIC_{15} was greater than the HIC_{36} which can be attributed to the shape of the resultant head acceleration profile. A rapid change in acceleration of the head of the altered model created a spike on the altered resultant head acceleration profile. The HIC_{15} evaluates the area under the acceleration curve for a 15 ms window and since the HIC equation has an exponential term (2.5), small differences in area under the curve create large differences in calculated values of the HIC. Conversely, the HIC_{36} was greater than the HIC_{15} for the unaltered model which again is attributed to the wider and shallower profile of the unaltered resultant head acceleration profile. All calculated maximum values for the HIC

were considerably less than the limiting values of 570 and 1000 for the HIC₁₅ and HIC₃₆ respectively as recommended by NHTSA.

6.3.7 Head Rotation

The degree of rotational displacement of the head of the altered model was 31 percent greater than that of the unaltered model. This difference can be attributed to reduced axial and angular stiffness material properties of the neck of the altered model. With reduced material stiffness properties, the neck of the altered model would provide less resistance to rotational displacement per given unit of acceleration. This explanation is consistent with the observation that the altered model exhibited a greater degree of rotational displacement than the unaltered model given the same acceleration input. The time to peak head rotational displacements were similar, 74 ms for the altered versus 70 ms for the unaltered which is to be expected since the prescribed acceleration pulse was identical for both models.

6.3.8 Head Trajectory

The altered model exhibited a greater local (x,z) coordinate system displacement as compared to the unaltered model. The altered model local x head excursion was 16 percent greater than the unaltered model. The rationale for the altered model exhibiting a greater degree of head trajectory is again due to the reduced stiffness of the neck which lends to a greater displacement. In addition, the head trajectory of the altered model more closely resembles the profile of the experimental pediatric cadaver sled test conducted by Kallieris et al. (1976). Exact comparisons can not be made between the altered model and the pediatric test due to advancements in child safety seat design, restraint systems

employed (i.e. 5-Point Harness) and anchorage methods (i.e. LATCH), however, there is no other known pediatric cadaver sled test to use as a baseline for comparison.

6.4 Hypotheses Revisited

6.4.1 Hypothesis 1

The neck of the Hybrid III three-year-old child finite element model is significantly stiffer than that of the pediatric cadaver cervical spine data.

Based on the findings of this research, the null hypothesis is rejected and the research hypothesis can be accepted.

The results of this study indicate that significant differences exist in the magnitude of linear and angular stiffness of the Hybrid III three-year-old finite element model as compared to pediatric cadaver data. This finding was consistent with previous research conducted by Sances et al. (2002) who found that the linear stiffness of the Hybrid III adult dummy under compressive loading was stiffer as compared to adult cervical spine specimens.

6.4.2 Hypothesis 2

The Hybrid III three-year-old child finite element model does not adequately predict the failure tolerance of the pediatric cadaver cervical spine data under axial tensile loading conditions.

Based on the findings of this research, the null hypothesis is rejected and the research hypothesis can be accepted.

The Hybrid III three-year-old finite element model greatly over predicted the failure tolerance of the pediatric cervical spine under axial tensile loading conditions.

6.4.3 Hypothesis 3

The Hybrid III three-year-old child finite element model does not exhibit the same kinematic response of the pediatric cervical spine data under flexion loading conditions.

Based on the findings of this research, the null hypothesis is rejected and the research hypothesis can be accepted.

The Hybrid III three-year-old finite element model over predicted the magnitude of the bending moment for flexion and extension as compared to pediatric cadaver data.

6.4.4 Null Hypothesisxx

There will be no difference in stiffness, failure tolerance or kinematic response under flexion between the neck of the Hybrid III three-year-old child finite element model and that of the pediatric cadaver cervical spine data.

Based on the findings of this research, the null hypothesis is rejected for each of the three research hypotheses.

7. CONCLUSIONS AND FUTURE WORK

7.1 Conclusions

The kinematics of the Hybrid III three-year-old child finite element model were compared to experimentally determined values of neck stiffness for a small population of pediatric cadaver specimens. Significant differences in stiffness were found. The material properties of the pediatric cadaver data were implemented into the Hybrid III model and the experimental procedure for the pediatric cadaver data was numerically simulated. Excellent prediction capabilities were observed. The kinematics of the altered and unaltered Hybrid III models under crash loading conditions were compared and significant differences were determined. In addition, comparisons between the altered and unaltered models were made with pediatric cadaver sled test results. Conclusions are summarized as follows:

1. The neck of the Hybrid III three-year-old finite element model is 435 times stiffer under axial tensile loading, 12.4 times stiffer under flexion bending loading and 4.8 times stiffer under extension bending loading conditions than that of recently obtained experimental pediatric cadaver data.
2. The altered Hybrid III model exhibits a 31 percent greater degree of head rotation than the unaltered model when subjected to a crash pulse which is more consistent with the degree of rotation of a child cadaver and other child dummy finite element models.
3. The altered Hybrid III model exhibits a 91 percent greater degree of chest deflection than the unaltered model when subjected to a crash pulse.

4. The altered Hybrid III model head trajectory more closely resembles the profile of the experimental pediatric cadaver sled test than the unaltered model. In addition, the altered model exhibited a 16 percent greater local x head excursion as compared to the unaltered model when subjected to a crash pulse which more closely resembles the local x head excursion of the pediatric cadaver sled test.
5. Overall, the altered Hybrid III model more accurately predicts the kinematics of the head and neck expected based on experimentally obtained pediatric cadaver data, in comparison to the original Hybrid III model.

7.2 Future Work

Future work should focus on making comparisons between other child dummy models such as the child finite element model with experimentally obtained pediatric cadaver data and potentially implement the pediatric cadaver data into the cervical spine of these models.

8. PUBLICATIONS RESULTING FROM THIS WORK

Kapoor, T., Altenhof, W. & Tot, M. (2007). Responses of the Q3, Hybrid III and a three year old child finite element model under a simulated 213 test. Abstract Accepted SAE World Congress and Exhibition. April 14-17, 2008, Detroit, MI, USA.

Kapoor, T., Altenhof, W., Tot, M. & Howard, A. (2007). Use of load limiting tethers in child restraint systems as a method to mitigate injuries to toddlers in frontal crash. Canadian Multidisciplinary Road Safety Conference. Montreal, Canada.

Kapoor, T., Altenhof, W., Tot, M., Zhang, W., Howard, A., Rasico, J., Zhu, F. & Mizuno, K., (2007). Load limiting behaviour in CRS tether anchors as a method to mitigate head and neck injuries to children in frontal crash. Traffic Injury Prevention. Article in Press.

Tot, M., Kapoor, T., Altenhof, W. & Marino, W. (2007). Implementation of child biomechanical neck behaviour into the Hybrid III crash test dummy. Abstract Accepted SAE World Congress and Exhibition. April 14-17, 2008, Detroit, MI, USA.

Wang, Q., Kapoor, T., Tot, M., Altenhof, W., & Howard, A. (2006). Countermeasures to alleviate injuries for three-year-old children in side impact crashes. International Journal of Crashworthiness. Article in Press.

Zhang, W., Kapoor, T., Tot, M., Altenhof, W., Howard, A. & Mizuno, K. (2007). A comparison of the kinematics and the head and chest injury parameters of the THUMS child model and the Hybrid III 3-year-old dummy in frontal crashes. SAE Paper No. 07M-139.

9. REFERENCES

- Andersen P. A. (1988). Occipital cervical instability associated with traumatic tears of the transverse ligament of the atlas. Orthopedic Transactions Abstracts, 12, 41.
- Anderson, P. A., & Montesano, P. X., (1992). Traumatic injuries of the occipital-cervical articulation, in Camins MB, Oleary PF (eds): Disorders of the Cervical Spine. Baltimore: Williams and Wilkins, 273-284.
- Arbogast, K. B., Cornejo, R. A., Kallan, M. J., Winston, F. K., & Durbin, D. R. (2002). Injuries to children in forward facing child restraints. Annual Proceedings of the Association of Advancement of Automotive Medicine 46, 212-230.
- Arbogast, K. B., Durbin, D. R., Cornejo, R. A., Kallan, M. J., & Winston F. K. (2004). An evaluation of the effectiveness of forward facing child restraint systems. Accident Analysis and Prevention 36 (4), 585-589.
- Bools J. C., & Rose, B. S. (1986). Traumatic atlantooccipital dislocation: two cases with survival. American Journal of Neuroradiology 7, 901-904.
- Brown, R. L., Brunn, M. A., & Garcia, V. F. (2001). Cervical spine injuries in children; a review of 103 patients treated consecutively at a level 1 pediatric trauma centre. Journal of Pediatric Surgery 36, 107-114.
- Brown, J. K., Ping, Y., Wang, S., & Ehrlich, P. E. (2006). Patterns of severe injury in pediatric car crash victims: Crash injury research engineering network database. Journal of Pediatric Trauma 41 (2), 362-367.
- Cassan B. F., Caillieret, M. C., & Tarriere, C. (1992). Les apports de la biomecanique a la securite des enfants a l'interieur des voitures. Annales de Pediatre 39 (3), 165-173.

Cassan B. F., Page, M., Pincemaille Y., Kallieris, D., & Tarriere, C. (1993). Comparative study of restrained child dummies and cadavers in experimental crashes. SAE Paper No. 933105.

Chazal, J., Tanguy, A., Bourges, M., Gaurel, G., Escande, G., Guillot, M., & Vanneville, G. (1985). Biomechanical properties of spinal ligaments and a histological study of the supraspinal ligament in traction. Journal of Biomechanics, 18, (3) 167-176.

Ching, R. P., Nuckley, D. J., Hertsted, S. M., Eck, M. P., Mann, F. A., & Sun, E. A. (2001). Tensile mechanics of the developing cervical spine. Stapp Car Crash Journal 45, 329-336.

Cirak, B., Ziegfeld, S., Knight, V. M., Chang, D., Avellino, A. M., & Paidas, C. N. (2004). Spinal injuries in children. Journal of Pediatric Surgery 39 (4), 607-612.

Copes, W. S., Sacco W. J., Champion, H, R., & Bain, L. W. (1990). Progress in characterizing anatomic injury. Journal of Trauma, 30 (10), 1200-1207.

Dai, L. Y., Ni, B., & Yuan, W. (1999). Pediatric cervical spine and spinal cord injuries. China. Journal of Pediatric Surgery 20, 96-98.

Desantis-Klinich, K., Saul, R. A., Auguste, S., Backaitis, M., & Kleinberger, M. (1996). Techniques for developing child dummy protection reference values. NHTSA Event Report, Docket Submission # 74-14 Notice 97 Item 069.

Dublin A. B., Marks, W. M., & Weinstock D. (1980). Traumatic dislocation of the atlanto-occipital articulation (AOA) with short-term survival. With a radiographic method of measuring the AOA. Journal of Neurosurgery 52, 541-546.

Duncan, J. M. (1874). On the tensile strength of the fresh adult fetus. British Medical Journal 19, 763-764.

Dupuis, R., Meyer, F., & Willinger, R. (2005). Three years old child neck finite element neck modelisation. Conference Proceedings, Louis Pasteur University. Paper number 05-0081.

Fuchs, S. M., Barthel M. J., Flannery A. M., & Christoffel, K. K. (1989). Cervical spine fractures sustained by young children in forward facing car seats. Pediatrics 84 (2), 348-354.

Gadd C.W. (1966). Use of a weighted-impulse criterion for estimating injury hazard. Conference Proceedings 10th Stapp Car Crash Conference. Holloman Air Force Base, NM, 95-100.

General Motors, Hybrid III Automotive Crash Test Dummies Have Roots in Aviation.http://www.gm.com/company/gmability/safety/protect_occupants/dummies/dummy_timeline_010702.html. Accessed On-line October, 2006.

Gennarelli, T. A. (1986). Mechanism and pathophysiology of cerebral concussion. Journal of Head Trauma Rehabilitation 1 (2), 23-29.

Gennarelli, T. A. Mechanisms of brain injury (1993). Emergency Medicine 11, 5-11.

Gray, H. (1860). Gray's Anatomoy Gray's Anatomy: Descriptive and Surgical. 2nd Ed. <http://education.yahoo.com/reference/gray/subjects/subject?id=73>. Accessed On-line October, 2006.

Hause, M., Hoshiro, R., Omata, S. (1974). Cervical spine injuries in children. Fukushima Journal of Medical Science 20 (1), 15-23.

Hendersen, M., Brown, J., & Paine M. (1994). Injuries to restrained children. Proceedings of the 38th Annual Association for the Advancement of Automotive Medicine, Lyon France, September 21-23, 1994.

Howard, A., McKeag, A. M., Rothman, L., Mills, D., Blazeski, S., Chapman, M., & Hale, I. (2005). Cervical spine injuries in children restrained in forward-facing child restraints: a report of two cases. Journal of Trauma 59, 1504-1506.

Huelke, D. F., Mackay, G. M., Morris, A., & Bradford M. (1991). A review of cervical fractures and fracture-dislocations without head impacts sustained by restrained occupants. Accident Analysis and Prevention. 25 (6), 731-743.

Janssen, E. G., Nieboer, J. J., Verschut, R., & Huijskens C. G. (1991). Cervical spine loads incuded in restrained child dummies. 35th Stapp Car Crash Conference, San Diego, CA. SAE Paper No. 912919.

Jones, N. (1989). Structural Impact. Cambridge University Press, Melbourne Australia.

Kallieris, D., Barz, J., Schmidt, G., Heess, G., & Mattern, R. (1976). Comparison Between Child Cadavers and Child Dummy by Using Child Restraint Systems in Simulated Collisions. 20th Stapp Car Crash Conference. SAE Paper 760815.

Kapoor, T., Altenhof, W., & Howard, A. (2005). The effect of using universal anchorages in child restraint seats on the injury potential for children in frontal crash. International Journal of Crashworthiness, 10 (3), 305-314.

Kapoor, T., Altenhof, W., Wang, Q., & Howard, A. (2006). Injury potential of a three-year-old hybrid III dummy in forward and reward facing positions under CMVSS 208 testing conditions. Accident Analysis and Prevention. 38, 786-800.

King, A. I. (2000). Fundamentals of impact biomechanics: Part I – biomechanics of the head, neck and thorax. Annual Review of Biomedical Engineering, 2, 55-81.

Kokoska, E. R., Leller, M. S., Rallo, M. C., & Weber, T. R. (2001). Characteristics of pediatric cervical spine injuries. Journal of Pediatric Surgery 36, 100-105.

Mallott, A., Parenteau, C., Arbogast, K., & Mari-Gowda, S. (1993). Sled test results using the Hybrid III 6 year old child in frontal crashes. SAE Paper No, 933105, 1993.

Mallot, A., Arbogast, K., Cooper, J., Murad, M., Ridella, S., Barnes, S., Kallan, M., & Winston F. (2003). Differences in airbag performance with children in various restraint configurations and vehicle types. 18th International Technical Conference on Enhanced Safety of Vehicles, Nagoya, Japan, 2003.

McGrory, B. J., Klassen, R. A., & Chao, E. Y. S. (1993). Acute fractures and dislocations of the cervical spine in children and adolescents. Journal of Bone and Joint Surgery 75, 988-995.

Menon, R., Arbogast, K., Cooper, J., Murad, M., Ridella, S., Barnes, S., Kallan, M., & Winston, F. (2003). Differences in air bag performance with children in various restraint configurations and vehicle types. 18th International Technical Conference on Enhanced Safety of Vehicles, Nagoya, Japan.

Mertz, H. J., Driscoll, G. D., Lenox, J. B., Nyquist, G. W., & Weber, D. A. (1982). Responses of animals exposed to deployment of various passenger inflatable restraint system concepts for a variety of collision severities and animal positions. Proceedings of 9th ESV Conference November 1-4, Published in PT31, SAE 826047.

Mohan, D., Bowman, B. M., Snyder, R. G., & Foust, D. R. (1979). A biomechanical analysis of head impact injuries to children. Transactions of the ASME. Journal of Biomechanical Engineering, (101), 4, 250-260.

Mousny M., Saint-Martin, C., Danse, E., & Rombouts, J. J. (2001). Unusual upper cervical fracture in a 1-Year Old Girl. Journal of Pediatric Orthopaedics 21, 590-593.

Myers, B. S., & Winkelstein, B. A. (1995). Epidemiology, classification, mechanism, and tolerance of human cervical spine injuries. Critical Reviews in Biomedical Engineering 23 (5&6), 307-449.

Myklebust, J. B., Pintar, F., Yoganandan, N., Cusick, J. F., Maiman, D., Myers T. J., & Sances A., Jr. (1988). Tensile strength of spinal ligaments. Spine, 13, (5) 526-531.

Nance, M. L., Elliott, M. R., Arbogast, K. B., Winston F. K., & Durbin, D. R. (2006). Delta v as a predictor of significant injury for children involved in frontal motor vehicle crashes. Annals of Surgery 243 (1), 121-125.

National Highway Traffic Safety Administration. (2003). Traffic safety facts research note, March 2006. Motor vehicle crashes as a leading cause of death in the United States. Accessed on line, October 2006.

Nightingale, R. W., Winkelstein, B. A., Knaub, K. E., Richardson, W. J., Luck, J. F., & Myers, B. A. (2002). Comparative strengths and structural properties of the upper and lower cervical spine in flexion and extension. Journal of Biomechanics 35, 725-732.

Nuckley, D. J., Hertsted, S. M., Eck, M. P., & Ching, R. P. (2005). Effect of displacement rate on the tensile mechanics of pediatric cervical functional spinal units. Journal of Biomechanics 38, 2266-2275.

Ouyang, J., Zhu, Q., Zhao, W., Xu, Y., Chen, W., & Zhong, S. (2005). Biomechanical assessment of the pediatric cervical spine under bending and tensile loading. Spine (30) 24, E718-E723.

Patel, J. C., Tepas, III J. J., Mollitt D. L., Pieper, P. & (2001). Pediatric cervical spine injuries: Defining the disease. Journal of Pediatric Surgery 36, 373-376.

Public Health Agency of Canada (1996). http://www.phac-aspc.gc.ca/publicat/meas-haut/mu_w_e.html Government of Canada. Accessed On-line October, 2006.

Roche, C. C., & Carty, H. (2001). Spinal trauma in children. Pediatric Radiology 31, 677-700.

Ryan M. D., & Henderson J. J. (1992). The epidemiology of fractures and fracture-dislocations of the cervical spine. Injury 23, 38-40.

Sances, Jr A., & Kumaresan, S. (2001). Comparison of biomechanical head-neck responses of Hybrid III dummy and whole body cadaver during inverted drops. Biomedical Sciences Instrumentation 37, 423-427.

Sances, Jr A., Carlin, F., & Kumaresan, S. (2002). Biomechanical analysis of head-neck force in Hybrid III dummy during inverted vertical drops. Biomedical Sciences Instrumentation 38, 459-464.

Sherwood C. P., Shaw C. G., Van Rooij L., Kent R. W., Crandall J. R., Orzechowski K.M., Eichelberger M. R., & Kallieris D. (2003). Prediction of cervical spine injury risk for the 6-year-old child in frontal crashes. Traffic Injury Prevention 4 (3), 206-213.

Sochor, M. R., Faust, D. P., Garton H., & Wang, S. C. (2004). Simulation of occipitoatlantoaxial injury using a MADYMO model. Conference Proceedings of the SAE World Congress, Detroit Michigan. SAE Technical Paper 2004-01-0326.

Statistics Canada (2003). http://142.206.72.67/02/02b/02b_003_e.htm
Government of Canada. Accessed On-line October, 2006.

Steinmetz, M. P., Lechner, R. M., & Anderson, J. S. (2003). Atlantooccipital dislocation in children: Presentation, diagnosis, and management. Neurosurgical Focus, 14 (2), 1-7.

Thomas, D. J., & Jessop, M. E. (1983). Experimental head and neck injury. Impact Injury of the Head and Spine, ed. Ewing et al., pp. 177-217. Springfield IL: Thomas

Transport Canada, Road Safety in Canada - An Overview
<http://www.tc.gc.ca/roadsafety/stats/overview/2004/menu.htm> Accessed October, 2006.

Turchi, R., Altenhof, W., Kapoor, T., & Howard, A. (2004). An investigation into the head and neck injury potential of three-year-old children in forward facing and reward facing child safety seats. International Journal of Crashworthiness 9 (4), 419-431.

Van Ee, C. A., Nightingale, R. W., Camacho, D. L., Chancey, V. C., Knaub, K. E., Sun, E. A., & Myers, B. S. (2000). Tensile properties of the human muscular and ligamentous cervical spine. Stapp Car Crash Journal 44, 85-102.

Versace, J. (1971). A review of the severity index. Proceedings of the 15th Annual Stapp Car Crash Conference, Coronado, California. Paper no. 710881., pp. 771-796. Warrendale, PA: SAE.

Weber, K. (1995). Rear-facing restraint for small child passengers. UMTRI Res Rev 25, 12-17.

Weber, K. (2002). Child passenger protection. Accidental injury: Biomechanics and Prevention. A. Nahum and J. Melvin. New York, Springer-Verlang.

Williamson, A., Irvine, P., & Sadural, S. (2002). Analysis of motor vehicle related fatalities involving children under the age of six years. Report for the motor accidents authority.

Wismans J. (2004). Vehicle Crashworthiness and Occupant Protection. Southfield MI: American Iron and Steel Institute.

Yannacome, J., Whitman, G., Sicher, L., & D'Aulerio, L. (2005). Analysis of Nij in simulated real-world crashes with a 3-year-old Hybrid-III. International Journal of Crashworthiness (11) 5, 443-447.

Yoganandan, N. S., Pintar, F., Maiman, D. J., Cusick, J. F., Sances Jr., A., & Walsh, P. R. (1996). Human head-neck biomechanics under axial tension. Medical Engineering and Physics 18 (4), 289-294.

Yoganandan, N., Pintar F. A., Kumaresan, S., & Gennarelli, T. A., (2000). Pediatric and small female neck injury scale factor and tolerance based on human spine biomechanical characteristic. Conference proceedings of IRCOBI, Montpellier, September 21-23.

Yoganandan, N. S., Kumaresan, S., Pintar F. A., & Gennarelli, T. A., (2002). Pediatric Biomechanics. Biomechanics and prevention. A. Nahum and J. Melvin. New York, Springer-Verlang.

10. APPENDICES

APPENDIX A

The Finite Element Method

$$\sum F = (m) \cdot (a) + (c) \cdot (v) + (k) \cdot (x)$$

Where:

m, c and k are material properties;

m = mass

c = viscosity

k = stiffness

(m) · (a) = inertial component

(c) · (v) = viscous component

(k) · (x) = dampening component

2nd Order Differential equation is an equation containing a variable and 2 of its derivatives.

LS-DYNA approximates to a, v and d to simultaneously solve coupled 2nd order differential equations that define the material properties for a number of finite elements.

APPENDIX B

The Abbreviated Injury Scale

The Abbreviated Injury Scale (AIS) provides a ranking of the severity of injury. Injuries are ranked on a scale of 1 to 6, with 1 being minor and 6 being an unsurvivable injury. The scale represents the threat to life associated with an injury and is not meant to represent a comprehensive measure of severity. The AIS is not an injury scale, in that the difference between AIS1 and AIS2 is not the same as that between AIS4 and AIS5 (Copes et al., 1990).

Injury	AIS Score
1	Minor
2	Moderate
3	Serious
4	Severe
5	Critical
6	Unsurvivable

11. VITA AUCTORIS

Miroslav Joseph Tot was born in Windsor Ontario Canada on August 14, 1975. He graduated High School from the Honourable W. C. Kennedy Collegiate Institute in 1995. From there, he went on to the University of Windsor where he obtained a Bachelor of Human Kinetics degree (Honours, Cooperative Education) in 2000. He is currently a candidate for the Master's degree in Human Kinetics at the University of Windsor and hopes to graduate in the summer of 2007.